University of Alberta

Study of UV/Chlorine Photolysis in regard to the Advanced Oxidation
Processes (AOPs)

by

Jing JIN

A thesis submitted to the Faculty of Graduate Studies and Research
in partial fulfillment of the requirements for the degree of

Master of Science

in

Environmental Engineering

Department of Civil & Environmental Engineering

©Jing JIN
Fall 2010
Edmonton, Alberta

Examining Committee

Dr. Mohammed Gamal El-Din, Department of Civil and Environmental Engineering

Dr. James R. Bolton, Department of Civil and Environmental Engineering

Dr. Yang Liu, Department of Civil and Environmental Engineering

Dr. Jonathan G. C. Veinot, Department of Chemistry

ABSTRACT

This thesis aims mainly at investigating the potential oxidizing abilities and possible applications of the UV/Chlorine process as an Advanced Oxidation Process (AOP).

Several organic compounds were used and added into the samples as challenging radical scavengers to investigate the possibilities of the UV/Chlorine process being used in the water and wastewater treatment industry. The UV/H_2O_2 process was selected as a reference, and experiments were carried out parallel; the results obtained earlier in the UV/Chlorine process were compared to those of the UV/H_2O_2 process.

Methanol was added into active chlorine solutions at both pH 5 and 10. The quantum yields for the degradation of active chlorine were calculated after the samples had been exposed to UV. Also the production of $\cdot OH$ radicals was calculated by determining the generation of formaldehyde. The $\cdot OH$ radical yield factors, which are significant in evaluating AOPs, were calculated both in the UV/Chlorine and the UV/H_2O_2 processes. In addition to methanol, *para*-chlorobenzoic acid (*p*CBA) and cyclohexanoic acid (CHA) were added to active chlorine solutions and to H_2O_2 solutions. The first-order reaction rate constants for the oxidation of *p*CBA and CHA using the UV/Chlorine process were calculated and compared to those of the UV/H_2O_2 process. This allowed an evaluation of whether or not the UV/Chlorine process might be efficient for the treatment of contaminated water samples containing *p*CBA and/or CHA.

Finally the thesis comes to a general conclusion about the efficiency of the UV/Chlorine process compared to that of the UV/H_2O_2 process.

TABLE OF CONTENTS

LIST OF TABLES

LIST OF FIGURES

ACRONYMS

AOPs   Advanced Oxidation Processes

AWWA   American Water Works Association

CHA   Cyclohexanoic acid

DBPs   Disinfection By-Products

LP   Low Pressure

OSPW   Oil Sands Process-affected Water

*p*CBA   *para*-chlorobenzoic acid

PAC   Photodegradation of Active Chlorine

THMs   Trihalomethanes

TOC   Total Organic Carbon

USEPA   US Environmental Protection Agency

UV   Ultraviolet

WHO   World Health Organization

CHAPTER 1 INTRODUCTION

This chapter briefly introduces the principal reactions and applications of several Advanced Oxidation Processes (AOPs) that are used in water and wastewater treatment processes. Compared to those AOPs, the properties and the potential applications of the UV/Chlorine process as an AOP are yet to be studied. The second part of the chapter enumerates the tasks and the objectives of this research.

1.1   Advanced Oxidation Processes in water and wastewater treatment

Advanced oxidation processes (AOPs) are defined as processes that are based on the generation of highly oxidative and reactive intermediates, such as hydroxyl radicals (·OH), at temperatures and pressures near ambient. They can be used as either stand-alone treatment processes or as pre-treatment or post-treatment processes. In Western Canada, where Oil Sands Process-affected Water (OSPW) has become a major environmental issue, the application of the AOPs for the treatment of OSPWs has been investigated to some extent.

Hydroxyl radicals, which are a key intermediate in AOPs, are much more powerful and reactive than other oxidants and can be used to oxidize organic pollutants in drinking water, wastewaters and industrial effluents. The relative oxidizing powers of various species are shown in Table 1.1.

Table 1-1 Relative oxidation power of various oxidizing substances (Oppenländer, 2003)

Oxidizing substance	Oxidation potential (V)
Hydroxyl radical ($\cdot OH$)	2.05
Atomic oxygen (O)	1.78
Ozone (O_3)	1.52
Hydrogen peroxide (H_2O_2)	1.31
Permanganate (MnO_4^{2-})	1.24
Chlorine (Cl_2)	1.00

Hydroxyl radicals can be generated from various processes. From the industrial aspect, however, it is very important to consider which approaches are most cost-effective in producing these intermediates with lower energy inputs.

There are several processes involving both chemical and photochemical reactions that can produce hydroxyl radicals, such as the Fenton reaction (Fe^{2+}/ H_2O_2), photo-Fenton reaction, photocatalysis, peroxone reaction (O_3/H_2O_2), ozone/activated carbon, UV/H_2O_2, UV/O_3, vacuum UV, ultrasound etc. Table 2-1 summarizes the principal reactions and reaction conditions for the major AOPs.

Table 1-2 Summary of the principal reactions occurring in various Advanced Oxidation processes (AOPs)

AOPs	Principal reactions	
Fenton Reaction	$Fe^{2+} + H_2O_2 \rightarrow FeOOH^+ + H^+$ $FeOOH^+ + H^+ \rightarrow Fe(OH)^{2+} + \cdot OH$ (Oppenländer, 2003)	pH = 3 The reactions are strongly dependent on pH
Photo Fenton Reaction	$H_2O_2 + Fe^{3+} \rightarrow Fe(O_2H)H^{2+} + H^+$ (Pignatello et al. 1999) $H_2O_2 + Fe(OH)^{2+} \rightarrow Fe(OH)(O_2H)^+ + H^+$ $Fe(O_2H)^{2+} + hv \rightarrow Fe^{2+} + HO_2\cdot$ $\cdot OH + H_2O_2 \rightarrow H_2O + HO_2\cdot$	Optimal pH = 3
Hydrogen Peroxide	$H_2O_2 + hv \rightarrow 2\cdot OH$	H_2O_2 only absorbs wavelengths below 280 nm. The absorption coefficient at 254 nm is only 18 M^{-1} cm^{-1}
UV/Ozone	$O_3 + hv \rightarrow O(^1D) + O_2(^1\Delta_g)$ $O(^1D) + H_2O \rightarrow H_2O_2$ $H_2O_2 + hv \rightarrow 2\cdot OH$	pH > 8
Photocatalysis	Photocatalyst $(TiO_2) + hv \rightarrow e^- + h^+$ $e^- + O_2 \rightarrow O^-_2$ $h^+ + organics \rightarrow CO_2$ $h^+ + H_2O \rightarrow \cdot OH + H^+$ $\cdot OH + organics \rightarrow CO_2$ (R. Thiruvenkatachari *et al.*, 2007)	
Vacuum UV	$H_2O + hv$ (Vacuum UV) $\rightarrow \cdot OH + H\cdot$	
Ultrasound	$H\cdot + H_2O \rightarrow H_2 + \cdot OH$	

The utilization of AOPs allows the destruction and mineralization of hazardous organic compounds from wastewater and process waters. When AOPs are applied, the appropriate one should be selected depending on the actual problem. For example, photocatalytic oxidation was be used in the treatment of OSPW. Lab-scale experiments have been carried out and have proven that this process can oxidize the organic and inorganic compounds in the OSTW (Bessa *et al.,* 1999). On the other hand, however, the photocatalysis process might not be safe for drinking water treatment process, since the

separation of titanium dioxide particles from the treated water after the process is still of concern. Also the photocatalysis process has a very low (4%) quantum yield for the generation of hydroxyl radicals. The Fenton process, as well, cannot be used for drinking water treatment, since it requires either a pH lower than 3, which is not an optimal pH for drinking water treatment process, or the existence of strong UV absorbing substances, which can be difficult to remove by the following treatment procedures. However, the Fenton peroxidation process can be quite effective in the reduction of sludge production and to improve the dewaterability of the sludge during the post-treatment of sewage sludge (Neyens *et al.,* 2002).

The Fenton process, ozone based AOPs, and the photocatalysis process have been found to be more effective in oxidizing pharmaceuticals and endocrine disruptors (EDCs) than the ozonation process alone, since the production of hydroxyl radicals is higher during these AOPs (Ikehata *et al.,* 2006). It should be noted that an important goal is to improve the biodegradability for the water and wastewater treatment processes and that complete mineralization of the toxic compounds is not necessary; this enables a wider application of AOPs due to their strong oxidizing abilities (Bessa *et al,* 1999).

1.2   Research Objectives

Excessive consumption of chlorine under direct sunlight was observed for swimming pools that use aqueous chlorine as a disinfectant. Nowell *et al.* (1992b) confirmed that the predominant active species from the UV/chlorine process is the ·OH radical. The production of ·OH radicals, when aqueous chlorine solutions are exposed to UV, has enabled the UV/Chlorine process to become a potential AOP.

Chlorine has been used as a disinfectant in drinking water treatment for more than a century and is still widely used. There have been increasing public health concerns about the disinfection by-products (DBPs) produced during chlorine disinfection and some pathogenic microorganisms that cannot be inactivated by chlorine, such as *Giardia spp.* and *Cryptosporidium spp.* The UV driven chlorine process, as an AOP, can be a solution to this issue to inactivate water born pathogenic microorganisms and also to destroy hazardous organic compounds in drinking water and wastewater.

This research is focused on studying chlorine photolysis driven by UV and the production of ·OH radicals after the addition of certain types of organic matter, and thus finding effective ways to remove organic contaminants from waste streams.

1.2.1 Production of ·OH radicals during the UV/Chlorine and the UV/H_2O_2 processes

Methanol was added to chlorine and hydrogen peroxide solutions which were then put under UV and exposed for certain period of time. The production of the ·OH radicals was determined by analyzing for the oxidation product, namely formaldehyde. Meanwhile, the quantum yields were calculated for both the processes. The generation of hydroxyl radicals during the UV/Chlorine process was compared to that of the UV/H_2O_2 process.

1.2.2 Oxidation of certain organic compounds using the UV/Chlorine process

Other than methanol, other organic compounds such as *para*-chlorobenzoic acid and cyclohexanoic acid (CHA) were added into the solutions to test the oxidation abilities of the UV/Chlorine process and were compared to those of the UV/H_2O_2 process. The

5

pseudo first-order reaction rate constants for reaction with ·OH radicals were calculated for the organics at various concentrations.

1.2.3   Comparison of the UV/Chlorine and the UV/H₂O₂ processes

The overall hydroxyl radical production rates, quantum yields, and the efficiencies of oxidizing various organic compounds were compared between the UV/Chlorine and the UV/H₂O₂ processes. Thus, the potential of the UV/Chlorine process becoming an AOP that could be applied in water and wastewater treatment industry was investigated.

1.3   References

Bessa, E., Sant Anna, G. L., and Dezotti, M. (2001). "Photocatalytic/H_2O_2 treatment of oil field produced waters." Applied Catalysis B-Environmental, 29(2), 125-134.

Bielski, B. H. J., Cabelli, D. E., Arudi, R. L., and Ross, A. B. (1985). "Reactivity of HO_2/O^{-2} Radicals in Aqueous Solution." Journal of Physical and Chemical Reference Data, 14(4), 1041-1100.

Ikehata, K., Naghashkar, N. J., and Ei-Din, M. G. (2006). "Degradation of aqueous pharmaceuticals by ozonation and advanced oxidation processes: A review." Ozone-Science & Engineering, 28(6), 353-414.

Neyens, E., and Baeyens, J. (2003). "A review of classic Fenton's peroxidation as an advanced oxidation technique." J. Hazard. Mater., 98(1-3), 33-50.

Nowell, L. H., and Hoigne, J. (1992b). "Photolysis of Aqueous Chlorine at Sunlight and Ultraviolet Wavelengths .2. Hydroxyl Radical Production." Water Res., 26(5), 599-605.

Oppenländer, T. (2003). *Photochemical Purification of Water and Air: Advanced Oxidation Processes (AOPs): Principles, Reaction Mechanisms, Reactor Concepts*, Wiley, New York.

Pignatello, J. J., Liu, D., and Huston, P. (1999). "Evidence for an additional oxidant in the photoassisted Fenton reaction." Environ. Sci. Technol., 33(11), 1832-1839.

Sun, L. Z., and Bolton, J. R. (1996). "Determination of the quantum yield for the photochemical generation of hydroxyl radicals in TiO_2 suspensions." J. Phys. Chem., 100(10), 4127-4134.

Thiruvenkatachari, R., Vigneswaran, S., and Moon, I. S. (2008). "A review on UV/TiO_2 photocatalytic oxidation process." Korean Journal of Chemical Engineering, 25(1), 64-72.

CHAPTER 2 RESEARCH ACHIEVEMENTS AND APPLICATIONS OF THE UV/CHLORINE PROCESS AS AN ADVANCED OXIDATION PROCESS – A REVIEW

In this chapter, fundamental aspects concerning the UV/Chlorine process as an Advanced Oxidation Process, including the principal reactions, quantum yield calculations, influencing factors, etc., are discussed. Also, the research achievements of the UV/Chlorine process and its applications in the water industry are illustrated.

2.1   The production of $\cdot$OH radicals

2.1.1   The photolysis of active chlorine

There are several basic reactions occurring during the production of $\cdot$OH radicals, as follows (Bolton, 2010):

[2.1] $Cl_2 + H_2O \rightarrow HOCl + HCl$

[2.2] $HOCl \leftrightarrow H^+ + OCl^-$ (equilibrium with $pK_a = 7.6$ at 20 °C)

[2.3] $HOCl + UV\ photons \rightarrow \cdot OH + Cl\cdot$

[2.4] $OCl^- + UV\ photons \rightarrow \cdot O^- + Cl\cdot$

[2.5] $\cdot O^- + H_2O \rightarrow \cdot OH + OH^-$
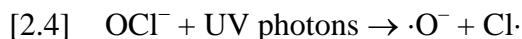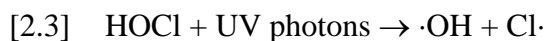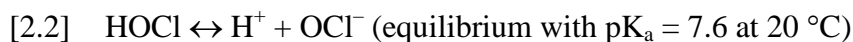
Also, there exist chain reactions that can lead to the further consumption of HOCl, as studied by Oliver and Carey (1970), who carried out a series of experiments around pH 4 using radical scavengers, such as ethanol, *n*-butanol and benzoic acid. They proposed the following chain reactions:

[2.6] $HOCl + UV \text{ photons} \rightarrow \cdot OH + Cl\cdot$

·OH radical chain reactions:

[2.7] $\cdot OH + RH \rightarrow \cdot R + H_2O$

[2.8] $\cdot R + HOCl \rightarrow RCl + \cdot OH$

·Cl radical chain reactions:

[2.9] $\cdot Cl + RH \rightarrow \cdot R + HCl$

[2.10] $\cdot R + HOCl \rightarrow ROH + \cdot Cl$

Thus more active chlorine may be consumed during the photolysis processes as a result of the above chain reactions. Giles and Danell (1983) indicated that 99% of chlorine was consumed in a municipal water treatment plant by UV-induced dechlorination. Zheng *et al.* (1999a) found that at the highest UV dose of 4825 mJ/cm^2 applied in a medium pressure (MP) UV reactor located upstream of a UV disinfection unit, the active chlorine demand was five times that of the condition without the UV process. The greater the UV dose applied, the higher was the active chlorine demand.

2.1.2 Quantum yield of the photodegradation of active chlorine

The fraction of excited states that leads to photochemistry is called the quantum yield (Φ) defined as follows:

Eq. (2.1)
$$\Phi = \frac{\text{moles of product formed or reactant removed}}{\text{einsteins of photons absorbed}}$$

Thus the quantum yield for the photodegradation of active chlorine[1] is defined as moles of active chlorine[2] decomposed per einstein[3] of UV photons absorbed by the sample. Theoretically, since one molecule corresponds to one photon absorbed when photochemistry happens, the quantum yield should never be higher than 1.0. However, when chain reactions occur, the quantum yield can be larger than 1.0 due to thermal reactions between ·OH radicals and the radical scavengers or reactions between ·Cl radicals and radical scavenging organic materials.

The photodegradation quantum yields observed by Buxton and Subhani (1972) in the photolysis of OCl⁻ ions at ambient temperature at 254, 313 and 365 nm were about 0.85, 0.39 and 0.6, respectively.

Also, they defined a yield factor η to describe the amount of ·OH radicals produced from active chlorine. This value could also be referred to as quantum yield of ·OH radicals, and is defined as:

---

[1] Free chlorine includes both hypochlorous acid (HOCl) and the hypochlorite (OCl⁻) ion. In this thesis, the term 'active chlorine' is used for these species.

[2] Each Cl_2 produces only one 'active Cl' (as one Cl_2 molecule decomposes into HOCl or OCl⁻ at pH 5 or 10, which are the pH values adapted in this research).

[3] One einstein is one mole (6.023×10^{23}) of photons.

Eq. (2.2) $$\eta = \frac{\Delta[\cdot OH]}{\Delta[\text{active Cl}]}$$

The consumption of active chlorine can be related to the consumption of other substances that can be used to generate ·OH radicals to calculate the quantum yields of ·OH radicals in other photolysis, for example, the quantum yield of ·OH radical generation in the UV/H_2O_2 process.

Nowell *et al.* (1992b) found the yield factors (η) for active chlorine photolysis at the wavelength 255 nm, where the photodegradation rate constants are almost the same for HOCl and OCl$^-$, were 0.1 and 0.85 at pH values of 10 and 5, respectively.

As described above, the quantum yield (Φ) is the fraction of excited states that lead to photochemistry. In the actual reactors, where the UV/Chlorine process takes place, it is not satisfactory that the rate constants can be expressed only in units of time^{-1}(Zepp, 1982), since it is hardly meaningful unless parameters, such as irradiance, absorbance and path length are given. Bolton and Stefan (2002) developed a protocol to calculate the quantum yields from 'fluence (UV dose)' based rate constant using a collimated beam apparatus.

In this approach, the photodegradation quantum yields for active chlorine can be calculated according to Bolton and Stefan (2002) as follows:

Eq. (2.3) $$k_1' = \ln\left(\frac{c_0}{c_F}\right)/F$$

Eq. (2.4) $$F = E_{op}'U_\lambda(\text{WF})(\text{DF})(\text{PF})(\text{RF})t = E_{op}'(\text{avg})U_\lambda t$$

Eq. (2.5) $$\Phi_C = 10\,k_1'U_\lambda/[\ln(10)\,\varepsilon_C]$$

Where:

Φ_C = the quantum yield of substance C

k_1' = the fluence based first-order 'rate constant' (m^2 J^{-1})

ε_C = the molar absorption coefficient (M^{-1} cm^{-1}) for substance C

C_0 and C_F = the initial and final concentrations of the substance under photolysis,

F = fluence (J m^{-2})

E_{op} = incident photon fluence rate (einstein s^{-1} m^{-2})

E_{op} (avg) = the average photon fluence rate in the solution

U_λ = molar photon energy (J einstein^{-1})

WF, DF, PF and RF are the water factor, divergence factor, Petri factor and reflection factor, accordingly, as defined by (Bolton and Linden, 2003).

The above equations enabled the calculation of the photodegradation quantum yields of active chlorine when oxidizing various organic compounds, and allow a connection between the quantum yields and the first order reaction rate constants.

2.2   Influencing factors for the photodegradation of active chlorine

There are several factors influencing the photodegradation of active chlorine, such as pH, temperature, and chlorine concentration, presence of organic matter and wavelength.

12

2.2.1 pH Effects

Photodegradation quantum yields of HOCl/OCl⁻ are significantly influenced by pH, arising from the pH dependence of hypochlorous acid HOCl and its conjugate base the hypochlorite ion OCl⁻. As described in Section 2.1.2, Nowell *et al.* (1992b) found that the yield factor (η) dropped from 0.85 to 0.1 when the pH increased from 5 to 10. This arises from the higher concentration of HOCl, which produces ·OH radicals, in the lower pH range. This is shown in Figure 2.1 for a hypochlorous acid solution with a concentration of 3 mM.
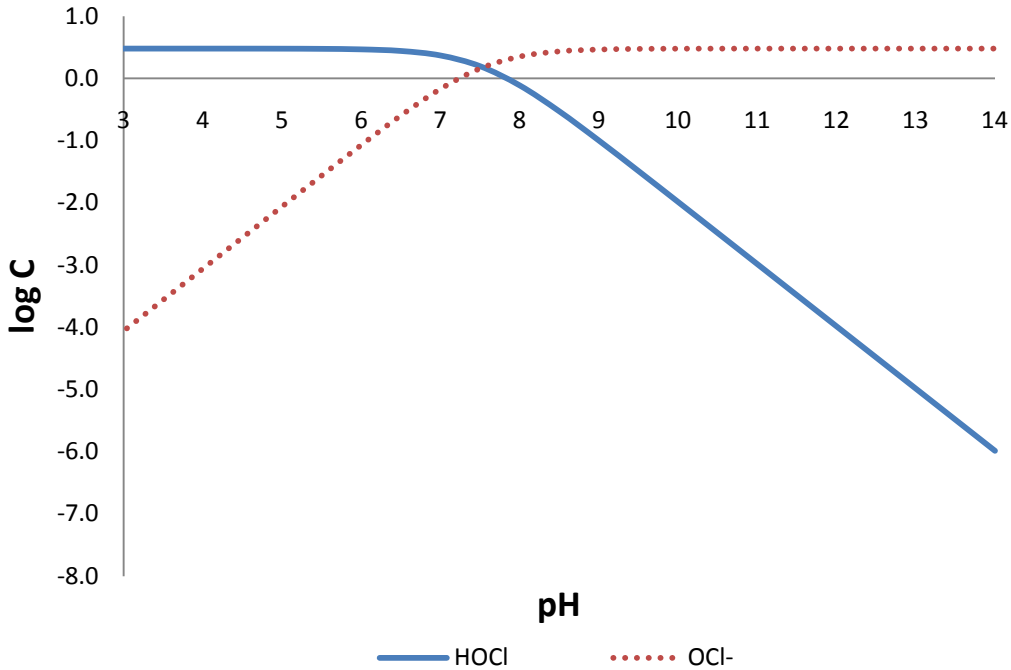
Figure 2.1 Logarithmic concentration diagram versus pH for 3 mM plot for hypochlorous (HOCl) acid

Figure 2.1 indicates that at low pH range, the predominant chlorine species is HOCl, while in the high pH range, the predominant species is the OCl⁻ ion.

The pH also affects the absorbance spectra of a chlorine solution, as shown in Figure 2.2. The molar absorption coefficients (M^{-1} cm^{-1}) of chlorine species at wavelengths between 200~400 nm were investigated (Feng, 2007). From this plot, HOCl has a peak absorbance at about 236 nm while OCl^{-} has peak absorbance at 292 nm (Feng, 2007). He also reported the molar absorption coefficients of HOCl and OCl^{-} to be about 101 M^{-1} cm^{-1} at 235 nm for HOCl and 365 M^{-1} cm^{-1} at 292 nm for OCl^{-}, using 15 chlorine solutions of different concentrations ranging from 3.5 to 100 mg/L.
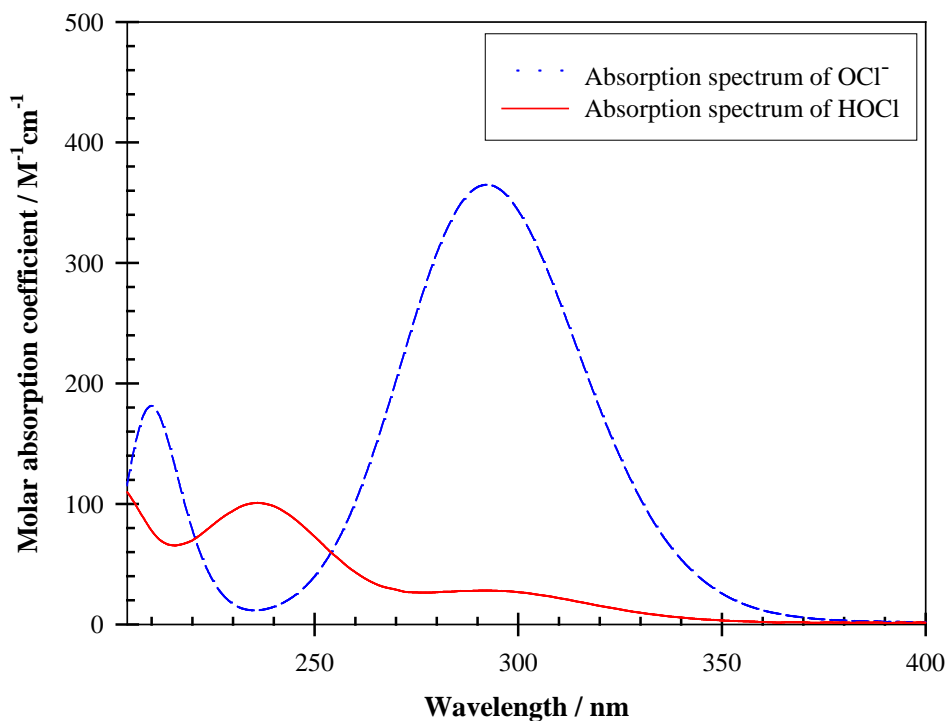
Figure 2.2 Absorbance spectra of HOCl and OCl^{-} measured at pH 5 and 10 at $21 \pm 2°C$ (Feng *et al.*, 2007)

He also reported the molar absorption coefficients for HOCl and OCl^{-} at 254 nm as 59 ± 1 and 66 ± 1 M^{-1} cm^{-1}, respectively. The molar absorption coefficients determined by Morris (1996) at 254 nm were 58 and 62 M^{-1} cm^{-1} for HOCl and OCl^{-}, respectively.

Thomsen *et al.* (2001) determined that molar absorption coefficient for OCl⁻ at 254 nm

was 60 M^{-1} cm^{-1}; however, Nowell *et al.* (1992b) reported different values, at 254 nm,

namely 155 and 121 M^{-1} cm^{-1} for HOCl and OCl⁻, respectively.

2.2.2   Concentration of active chlorine

The photodecomposition of active chlorine is also affected not only by the pH of the

solution, but also by the concentration of active chlorine.

The rate (R_{Cl}) of the photochemical reaction of active chlorine can be expressed as

(Bolton, 2010):

Eq. (2.6) $$R_{Cl} = \frac{GF_{Cl}\Phi_{Cl}}{V}$$

where:

G = incident photon flow (einstein s^{-1})

$F_{Cl} = f(\lambda)\,\chi_{Cl}$ = fraction of light absorbed by active chlorine[1]

$f(\lambda)$ = the total fraction of UV absorbed at wavelength λ and is given by

$1 - 10^{-A(\lambda)}$

χ_{Cl} = the fraction of the absorbed photons that are absorbed by active chlorine

$A(\lambda)$ is the total absorbance of the solution at wavelength λ.

Φ_{Cl} = photodegradation quantum yield of active chlorine

V = volume (L) of the solution

[1] The amount of available chlorine present as aqueous molecular chlorine, hypochlorous acid, and hypochlorite ion.

When the fraction of light absorbed by active chlorine is < 0.1, $f(\lambda)$ can be expanded in a Taylor series and F_{Cl} can be reduced to:

Eq. (2.7) $$F_{Cl} = \ln 10 \; \varepsilon_{Cl} \; C_{Cl} \; l$$

Thus, R_{Cl} can be reduced to:

Eq. (2.8) $$R_{Cl} = \frac{G\Phi_{Cl}}{V} \ln(10) \; \varepsilon_{Cl} \; C_{Cl} \; l$$

where:

ε_{Cl} = molar absorption coefficient (M^{-1} cm^{-1}) of active chlorine in the ambient solution

C_{Cl} = concentration of active chlorine in the solution

l = path length (cm)

According to Eq. (2.6), when F_{Cl} is near unity, the reaction kinetics of active chlorine photodecomposition approaches zero order, and thus the rate is independent of the chlorine concentration. Eq. (2.7) is valid only when the chlorine concentration is low, and the F_{Cl} value is below 0.1. In this case, the rate of photodecomposition changes to 'first-order' kinetics, and the rate becomes dependent on the chlorine concentration.

Also, the concentration of active chlorine seems to affect the photodegradation quantum yield. Feng *et al.,* (2007) reported that when the chlorine concentration is below 70 mg L^{-1}, the photodegradation quantum yield of HOCl is nearly constant at 1.0 as shown in Figure 2.3(a); When the concentration ranged from 70 to 1350 mg L^{-1}, the quantum yield increased with a slope of 0.0025 (mg Cl/L)$^{-1}$, as shown in Figure 2.3 (b), and the

quantum yield rose to approximately 4.5. In contrast, the photodegradation quantum yield of OCl$^-$ did not seem to be affected by the active chlorine concentration at all, and stayed at about 0.9 when the concentration ranged from 3.5 to 640 mg L^{-1}.
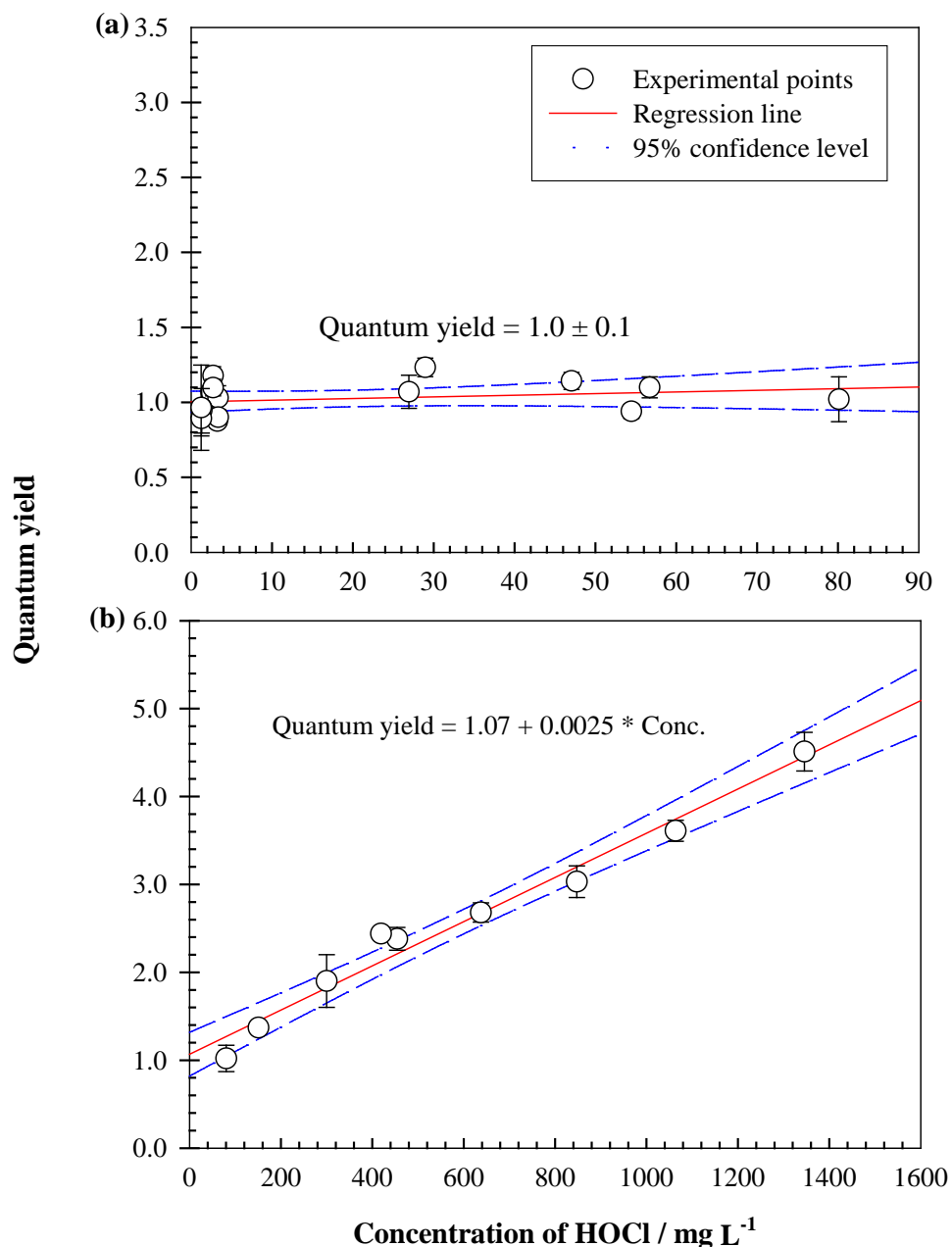
Figure 2.3 Quantum yields of the photodegradation of active chlorine (HOCl) at pH 5 and ambient temperature ($21 \pm 2°C$): (a) quantum yields determined when the concentration is lower than 70 mg L^{-1} and (b) quantum yields determined when the concentration is higher than 70 mg L^{-1} (Feng et al., 2007)

Apparently, for the photodegradation of HOCl, a chain reaction occurs, since the quantum yield rises above 1.0 (as discussed in Section 2.1.1).

2.2.3 The presence of organic matter (TOC)

Depending on the raw water quality, the presence of organic matter can be a factor of considerable influence on the photodecomposition of active chlorine.

The presence of certain organic matter has significant effects on the photodegradation quantum yield of HOCl, while, for OCl$^-$, no significant effects were observed. At pH 5, where HOCl dominates, the quantum yield gradually rises from 1 to approximately 50 when the methanol concentration increases from 0 to 120 mM, and there is a linear correlation between methanol concentration and the quantum yield (Feng, 2007).
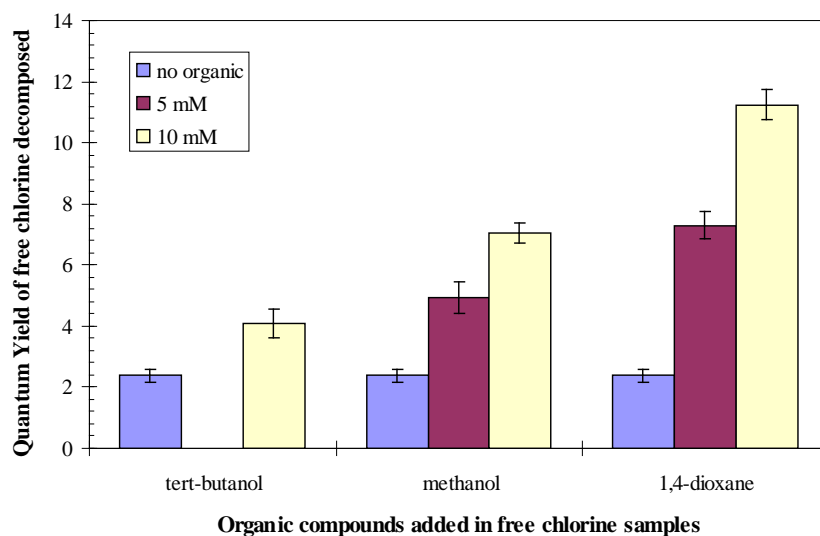
Figure 2.4 Comparison of the effects of three different organics on the photodegradation quantum yield of active chlorine (6.0 mM) at pH 5 and ambient temperature ($21 \pm 2°C$) (Feng *et al.*, 2007)

However, he found that at pH = 10, where OCl$^-$ dominates, the effect of methanol was minimal, since the quantum yield was 1.2 ± 0.2, regardless of changes in the methanol

18

concentration. Figure 2.4 shows the effects on the quantum yield at various levels of organic matter, such as tert-butanol, methanol and 1, 4-dioxane.

Except for concentration of specific organic compounds, the TOC concentration also affects the photodegradation quantum yield. For example, the quantum yield for an active chlorine concentration of 3.0 ± 0.2 mg/L changed from 1.1 to 4.9 when the TOC concentration increased from 0.4 to 6.8 mg/L. It was also found that and there exists a linear relationship between the TOC concentration and the quantum yield.

2.2.4 Temperature Effects

There have been several scholars debating temperature has influences the photodegradation quantum yield of active chlorine.

Feng *et al.,* (2007) found that no obvious change in the photodegradation quantum yield could be observed for the case of DI water, since the quantum yield stayed at approximately 1.0 when the temperature changed from 2 to 22 °C. Thus, temperature effects on the quantum yield for water containing a low TOC concentration can be neglected. However, for water samples containing 3.4 mg/L of TOC, the quantum yield dropped from 3.4 to 1.7 when temperature changed from 22 to 2 °C. Thus, the presence of TOC caused a temperature dependence in the rate of the photodegradation of active chlorine. This probably arises from the temperature dependence of chain reactions that occur in the case of elevated TOC concentrations.

2.2.5 Wavelength Effects

Since the energy of the photons and also the molar absorption coefficient of active chlorine are different for various wavelengths, the photolysis of active chlorine is

susceptible to the wavelength of UV. For example, Rahn *et al.* (2003) found that when the wavelength was changed from 254 nm to 284 nm, the quantum yield of the iodide-iodate chemical actinometer decreased from 0.8 to 0.3. Also, Buxton and Subhani (1972) found that the photodegradation quantum yield of OCl^- changed from 0.85 to 0.39 when the wavelength increased from 254 nm to 313 nm. This was very consistent with the results in the research carried out by Feng *et al.,* (2007), who showed that the photodegradation quantum yields of active chlorine solutions with a concentration around 3.0 mg/L at pH 8.0 varied from 0.96 ± 0.14 to 0.39 ± 0.07 when changing the wavelength from 254 nm to 300 nm. The irradiance that was used to calculate the quantum yields was measured by a UV radiometer (International Light, Model IL 1400A) calibrated at 254 nm. In addition, Watts et al. (2007) showed that the rate of HOCl photodegradation at pH 4 is greatly enhanced by MP UV, as compared to solutions exposed to 254 nm UV.

Feng *et al.,* (2007) also determined the photodegradation quantum yields for the same active chlorine samples introduced in the paragraph above (active chlorine concentration 3.0 ± 0.3 mg L^{-1} at pH 8.0 ± 0.3) exposed to various wavelengths from 220 to 300 nm. This time, however, the irradiance was measured by the ferrioxalate actinometer. As shown in Figure 2.5, the wavelength of the UV had minimal effects on the photodegradation quantum yield of active chlorine. The quantum yield measured was 0.9 ± 0.15 in that wavelength range. This inconsistency might be due to the irradiance values measured by the two methods: the ferrioxalate actinometer method and the radiometer method. Feng *et al.,* (2007) proved that the irradiance by the two methods above differed

20

because the correction factor[1] increases from 1 when the wavelength varied from around 254 nm to the values far away from 254 nm. This is due to the insensitivity of the radiometer to the wavelengths much larger than 254 nm.
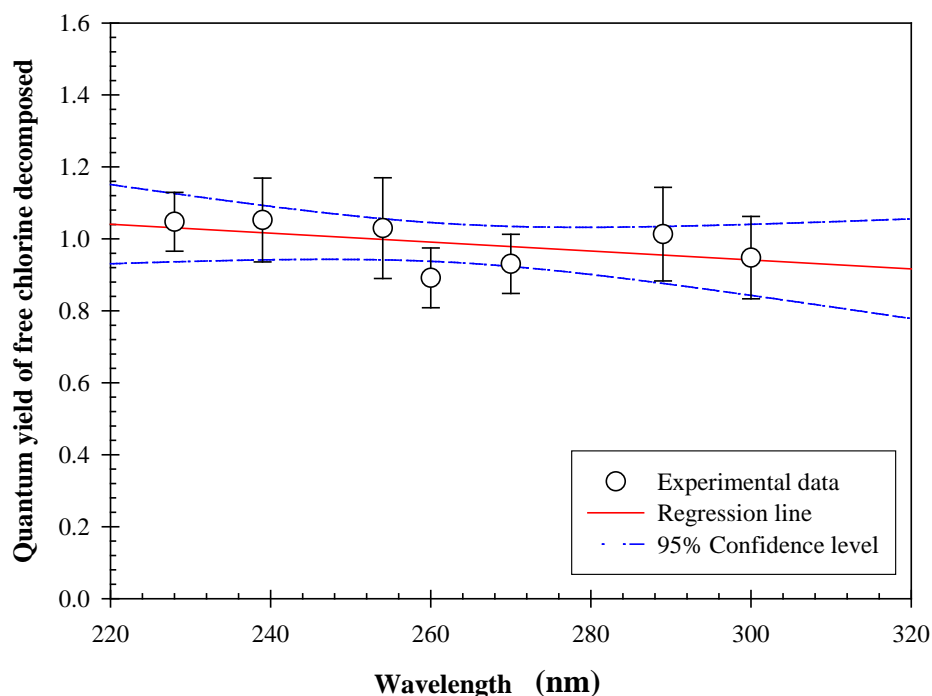
Figure 2.5 Quantum yield of free chlorine in different wavelength of UV (quantum yield measured based on the irradiance measured by the ferrioxalate actinometer) (Feng *et al.,* 2007)

According to the third law of photochemistry, that is, the energy of an absorbed photon must be equal to or greater than the weakest bond in the molecule, the photodegradation quantum yield of active chlorine should not be dependent on the wavelength of the UV, since there is only one lowest excited energy state for chlorine molecules. That is, as long as the wavelength meets the energy requirement, the quantum yield of the photochemical reaction should be independent of the wavelength. The wavelength dependence of the

---

[1] Correction factor is the ratio of the irradiance determined by ferrioxalate actinometer and the irradiance measured by the radiometer.

photodegradation quantum yield of active chlorine may turn out to be due to the irradiance measured by various experimental methods.

2.3 Research achievements and applications of the UV/Chlorine process as an Advanced Oxidation Process

Due to its ability to produce ·OH radicals, the UV/Chlorine process could be used as one of the AOPs in the water/wastewater treatment industry. Watts *et al.,* (2007) studied the decomposition of certain organic compounds using the UV/Chlorine process and compared it to the UV/H_2O_2 process. They pointed out that the UV/Chlorine process might become an alternative treatment method to the UV/H_2O_2 process. Also, by studying the photodegradation of active chlorine (PAC) under UV exposure (Feng *et al*., 2010) developed a new method to validate UV reactors. Compared to biodosimetry tests or chemical actinometry methods, the PAC method saves time and cost, is easier to operate, and its accuracy is equivalent to that of biodosimetry tests.

Despite its promising application in the future, the application of the UV/Chlorine process might be limited, since the UV dose delivered into the water might be lowered due to the added absorption and photochemical reactions of chlorine species. Örmeci *et al.* (2005) reported that a reduction of the log inactivation in UV disinfection was observed for chlorinated waters and waters containing monochloramine residuals. This effect arose from the absorption of UV by the disinfectants. In later studies, Watts *et al.* (2007) and Feng *et al.,* (2007) also studied the photochemical behaviour of chlorine species such as NH_2Cl, $HOCl$, and OCl^- under UV exposure. Cassan *et al.* (2006) investigated the photodecomposition of other chlorine species, such as THMs. These studies not only enabled the evaluation of the impacts of the photodecomposition of chlorine species on

22

the UV system performances, but also provided information about the impacts of those photochemical reactions on the water quality of chlorinated water bodies, such as indoor swimming pools.

2.3.1 Chlorine photolysis used as an Advanced Oxidation Process (AOP)

As discussed above, since the UV/Chlorine process is efficient in producing ·OH radicals, which are the major reactive intermediates in AOPs, the process could also be used as a technology to destroy organic contaminants in water/wastewater treatment processes.

Watts *et al.,* (2007) studied the decomposition of *para*-chlorobenzoic acid (*p*CBA) and nitrobenzene (NB) using the UV/Chlorine process. To obtain the steady-state ·OH radical concentration ([OH]$_{ss}$), Watts *et al.,*(2007) used the ·OH reactive probe compounds *p*CBA and NB in buffered solutions at active chlorine concentrations from 1–4 mg L^{-1}. The rate constants of the probes reacting with ·OH radicals were $k_{OH\text{-}pCBA} = 5 \times 10^9$ M^{-1} s^{-1} and $k_{OH\text{-}NB} = 3.9 \times 10^9$ M^{-1} s^{-1}. Buxton *et al.* (1988), Han *et al.* (2002), and Nowell and Hoigne (1992b) reported that the direct photolysis of *p*CBA and NB was insignificant when using LP UV lamps (UV$_{254}$). Thus, the self-decay of the *p*CBA and NB probes can be neglected. Except for the possible self-decay of the probes, the possibility of reactions between the probes and Cl· should be taken into account. Nowell and Hoigne (1992b) reported that no NB degradation could be observed in the solution due to Cl· radicals, and the NB was reported to be solely ·OH selective, while the degradation of *p*CBA was observed in the solution. The reported fluence-based pseudo first-order reaction rate constant of 3 mg·Cl/L and 2 μM of *p*CBA with a MP UV lamp was 5.67×10^{-4} cm^2 mJ^{-1} around pH 1. Since Nowell and Hoigne (1992b) also indicated

23

that the predominant photooxidant produced was the ·OH radical, the rate of Cl·

generation and reaction with pCBA at pH values larger than 1 can be neglected. Thus the

rate of degradation of pCBA/NB can be expressed as:

$$\frac{d[p\text{CBA}]}{dt} = -k_{\text{OH}-p\text{CBA}}[\text{OH}]_{ss}[p\text{CBA}]$$

The pseudo first-order fluence-based rate constants for pCBA and NB degradation for pH

4, 7.5 and 10.7 solutions of active chlorine and probes are shown in Figure 2.6.
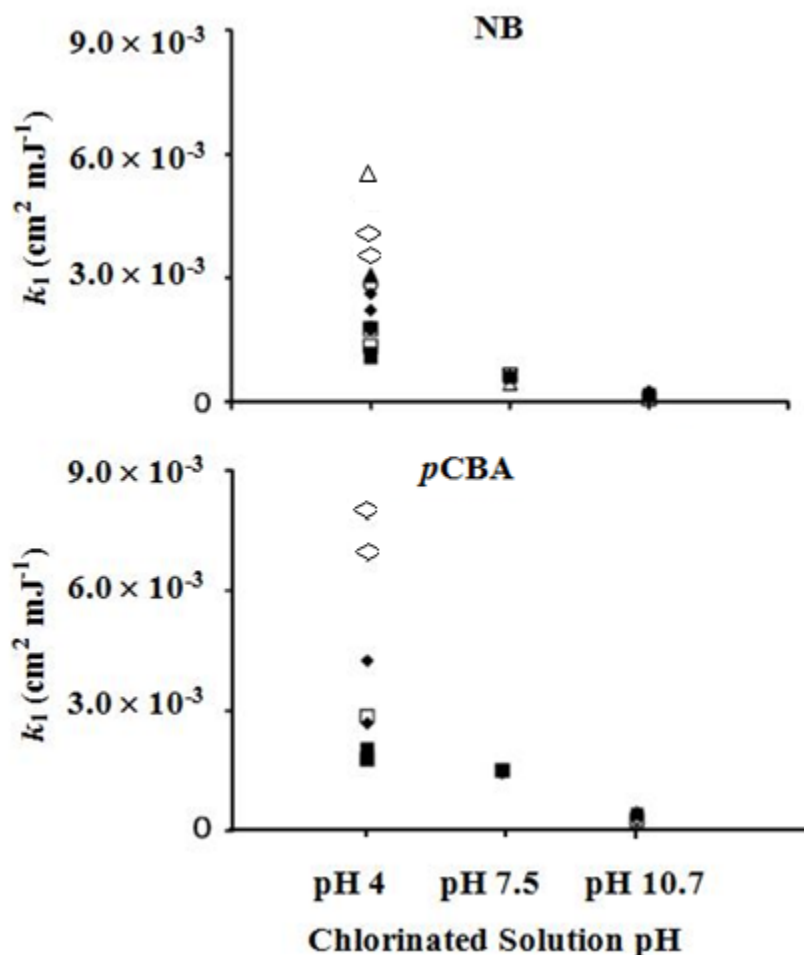
Figure 2.6 First-order fluence-based rate constants, k_1' ($\text{cm}^2 \text{ mJ}^{-1}$), for radical scavenger removal in solutions with varying doses of active chlorine; LP (1—□, 2—○, 3—◊, and 4 mg L^{-1} active chlorine--Δ) and MP (1—■, 2—●, 3—◆, and 4 mg L^{-1} active chlorine—▲) UV (Watts *et al.,* 2007)

24

From the pseudo first-order fluence based rate constants obtained above and the ·OH

radical formation rate, which is already known, the steady-state concentration of ·OH

radicals [·OH]$_{ss}$) can be calculated. Watts *et al.* (2007) reported that the ·OH radical

scavenging rate constant k_{OH} (due to reaction between ·OH and HOCl) is 8.46×10^4

$M^{-1} s^{-1}$, and the photodegradation quantum yield is 1.4 ± 0.2. When compared to the

UV/Chlorine process, the scavenging rate constant for the reaction of ·OH radicals being

scavenged by H_2O_2 forming water and ·HO$_2$ was $2.7 \times 10^7 M^{-1} s^{-1}$ (Buxton *et al.,* 1988),

and the quantum yield was 1.0 (Baxendale and Wilson, 1957). It is obvious that the

UV/Chlorine process has a smaller scavenging rate for the production ·OH and a larger

quantum yield, which is indicative that the UV/Chlorine process might be a potential

alternative to the UV/H_2O_2 process.

2.3.2   The Photodegradation of Active Chlorine (PAC) method used in the validation of the fluence delivered in UV reactors

Ultraviolet disinfection has been widely adopted as a cost-effective technology for the

inactivation of pathogenic microorganisms in drinking water treatment processes.

However, from the aspect of the design and implementation, one requires an effective

method to evaluate the delivery of UV dose (fluence) by the UV reactors. As required by

the USEPA, a biodosimetry test must be used in the validation of UV reactors in full-

scale plants (USEPA, 2006); however, this method is expensive, difficult to apply and

time-consuming.

Several researchers (Blatchley and Hunt, 1994; Nieminski et al., 2000; Mamane-Gravetz

and Linden, 2004) tried to improve the feasibility of biodosimetry testing. They

suggested that indigenous aerobic spores, which are naturally occurring in unfiltered water sources, could be used as an alternative indicator for the validation tests of UV reactors. Although this method largely reduced the effort for preparing the challenge microorganisms, it also had several short-comings, and the reduction equivalent fluence (REF) determined by this method proved to have a higher error level than that of a biodosimetry test. The disadvantages are: the indigenous spores are usually more resistant to UV, and the method can be largely affected by the quality of source water.

In addition to the biodosimetry test, there are also chemical actinometry methods, such as the uridine method (Linden and Darby 1997), the iodide/iodate method (Jin et al., 2006), and the ferrioxalate method (Quan et al., 2004), which have been developed to measure the fluence delivered in UV reactors. However, the chemicals used in the chemical actinometry methods are quite expensive which has limited the development of these methods. Also the actinometer solution, such as that for the KI/KIO_3 actinometer, is chemically unstable and needs to be prepared just before application. Furthermore, the addition of those chemicals affects the influent water quality and also affects the absorption characteristics of the water.

The fluence (UV dose) delivered by a UV reactor can be measured efficiently by the Photolysis of Active Chlorine (PAC) method. Since active chlorine keeps degrading while travelling within the reactor, the fluence delivered can be measured by the decrease in the chlorine concentration and the photodegradation quantum yield of active chlorine, and can be obtained by the Eq. (2.3) and Eq. (2.5). The C_0 and C_F in the equations would be the active chlorine concentrations (mg L^{-1}) at time 0 and F under exposure to UV.

By this method, the investigator only needs to measure the photodegradation quantum yield of active chlorine decomposed and the decrease in the chlorine concentration between the influent and effluent test water samples, which is quite feasible.

Feng *et al.,* (2010) carried out both the biodosimetry method and the PAC method in a bench scale UV system (flow rate $4 - 9 \text{ min}^{-1}$) for the validation of UV reactors and compared the results obtained from both methods.

During the test, the active chlorine degraded and, by mass balance, the photodegradation products were approximately 70 to 80% as chloride and 20% to 30% as chlorate. According to the results of the study, there is no significant influence from the TOC in the water samples, the UV transmittance, and the flow rate in the reactor. However, the interaction of temperature and the organics present in the water samples has a significant impact on the photodegradation quantum yield of active chlorine. Finally, the UV dose delivered in the reactor, as determined by the PAC method, was quite close to that determined by the biodosimetry method, as shown in Figure 2.7.
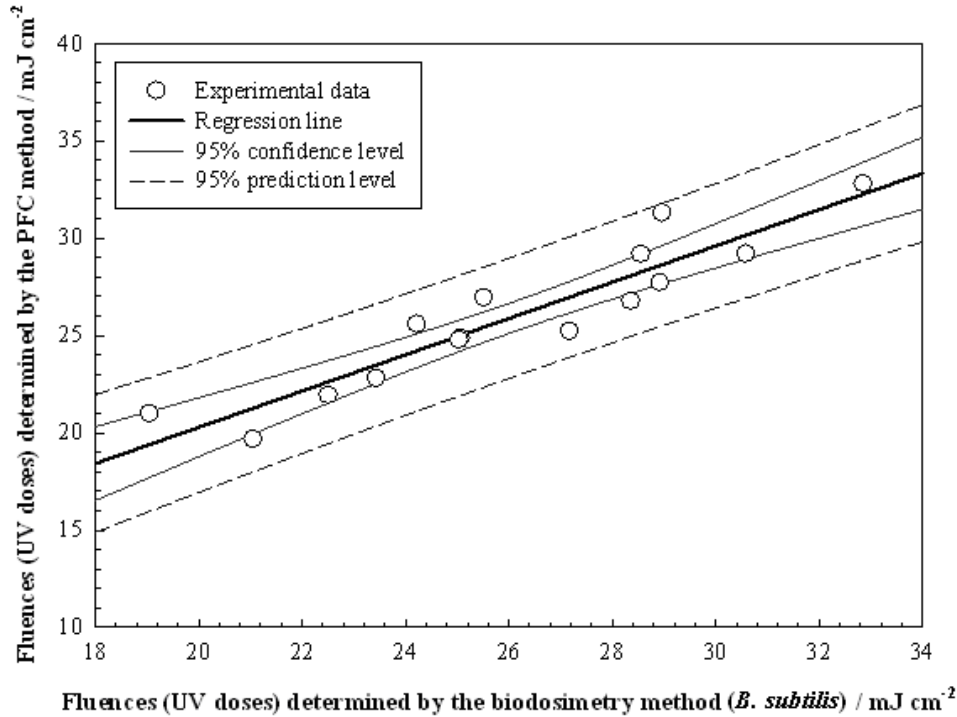
Figure 2.7 Correlation of the fluences (UV doses) determined by the PFC method and the biodosimetry method (Feng *et al.,* 2010)

Although the results shown in the study indicated that is no obvious difference between the biodosimetry and the PAC methods, the PAC method still has to be operated in a full-scale plant to verify the efficiency of the method.

2.3.3 The impacts of photochemical reactions of chlorine species on the UV disinfection system performance

Despite the oxidation power of the UV/Chlorine process, there are still concerns about the delivery of UV in UV disinfection systems arising from the photolysis of the disinfectants that will consume UV, the reduction in the UV transmittance and the possible formation of DBPs. Örmeci *et al.* (2005) carried out a study on the impacts of the photochemistry of disinfectants on the delivery of UV dose and the performance of the UV disinfection system. In this study, 'treated' water and deionized water were used

in LP and MP reactors to evaluate the system performance. The treated water was collected from the effluent of the sedimentation basin after the process of coagulation/flocculation prior to filtration. Although pre-filtered water is not generally used for UV disinfection; however, considering that the goal of the study was to evaluate the UV disinfection efficiency in the disinfection process, the 'treated' water could be used as a source. The 'treated' water samples were transferred to the laboratory within 15 min, stored in the dark and used during the experiments at a constant temperature of 4 °C.

Chlorine and monochloramine were added as disinfectants during the study. Results from the study (Örmeci *et al.,* 2005) indicated that the addition of chlorine and monochloramine prior to the UV disinfection increases the UV absorbance and therefore decreases the UV dose actually received by the water samples. However, the decrease was small, namely a 1% reduction for active chlorine and 2.5% reduction for monochloramine.

During the study, simulations were made for LP and MP UV reactors to evaluate the overall disinfection. When exposed to monochromatic UV [low pressure (LP) UV lamp] for the 'treated' water samples, the addition of 1 mg/L chlorine residual reduced the log removal of MS2 coliphage by 2%, and an increase of the chlorine residual to 3 mg/L did not significantly change the reduction in log removal. Also, in the case of monochloramine, the reduction of log inactivation was 4% both when the concentration was 1 or 3 mg/L; the reduction in this case was higher than in the case of chlorine.

In the case of a MP lamp, the reduction in the log inactivation was more drastic for the addition of a chlorine residual. A 14% log reduction was found after the addition of 1

mg/L chlorine residual and 9% log reduction was observed when the chlorine addition

was 3 mg/L. The lower log reduction when the chlorine residual was higher was due to

the absorbance in the wavelength between 245 and 260 nm, which was lower when the

treated water contained a 3 mg/L chlorine residual, as shown in Figure 2.8, though this is

difficult to see in the graph.
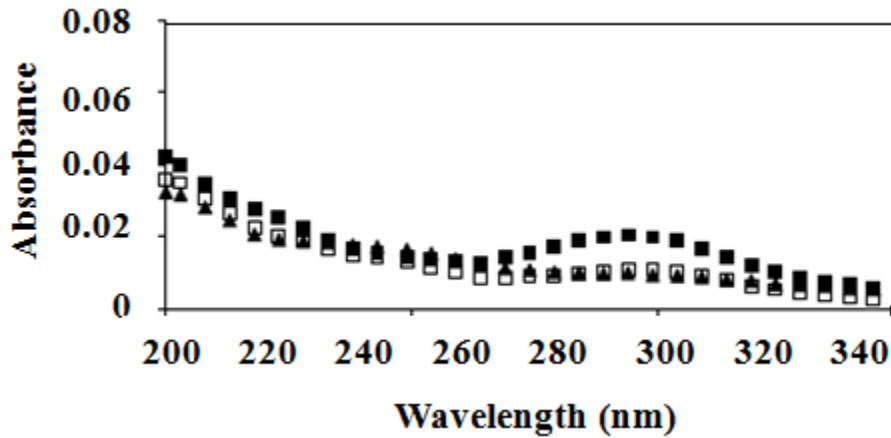
Figure 2.8 Absorption spectra of treated water at chlorine residual dose of 1 (▲), 3 (□),
and 5 (■) mg/L (Örmeci *et al.,* 2005)

In the case of a monochloramine residual, when the concentration was 1 mg/L, the

reactor displayed a 2% reduction in the log removal, while for a 3 mg/L residual, a

reduction of 14% was observed. As shown in Figure 2.9, there is a much higher

sensitivity of monochloramine at higher residual concentrations to UV between the

wavelengths of 230 and 275 nm, which is in the high absorption range of nucleic acids.
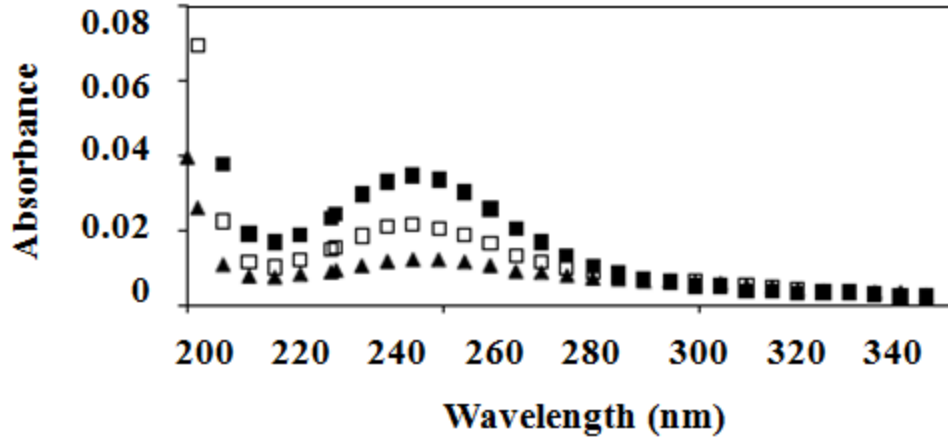
Figure 2.9 The absorption spectra of treated water at monochloramine residual dose of 1 (▲), 3 (□), and 5 (■) mg/L (Örmeci *et al.,* 2005)

This study indicated that the chlorine or monochloramine residual might not significantly affect the delivered UV dose; however, the disinfection performance could be influenced. Also, no significant reduction in log inactivation was observed when the samples were exposed to a LP UV lamp. When MP UV reactors were utilized, the disinfection performance largely depended on the raw water quality. When the concentration of organic matter is high, the addition of chlorine or chloramines tends to hinder the system performance by oxidizing the UV absorbing organic matter and thus the absorbance of the water sample decreases. In other cases, the system performance was enhanced due to the oxidation of organic matter inducing an increase in the UV transmittance.

At that time, the study did not indicate any inner photochemical reactions that might be happening when the disinfectants are exposed to UV, which could possibly influence the whole UV disinfection system. Also, the comparison of the UV absorbing properties of monochloramine and active chlorine was not yet accomplished. Further studies have to be carried out to study the impact of disinfectant residuals on UV systems.

31

2.3.4 The photolysis of free chlorine species and the impacts of UV on the water quality of chlorinated swimming pools

Swimming pools use chlorine as a disinfectant to remove microbiological pollutants within the bathing water. Today, UV is used more and more for the disinfection of swimming pools.

Swimming pools contain organic compounds, microorganisms, viruses and nitrogenous substances, such as urea, perspiration and cosmetics from bathers and swimmers. These compounds, when released into water, react with active chlorine, and can form DBPs, such as combined chlorines and trihalomethanes (THMs). Chloramines can cause respiratory problems, ocular and skin irritation (Henry *et al.*, 1995; Massin *et al.*, 1998) in human bodies, and THMs are carcinogenic. The formation of THMs, without UV treatment, can be greatly influenced by the amount of active chlorine present (Montiel, 1980; Judd and Jeffrey, 1995; Kim *et al*., 2002), and also by the TOC concentration within the water (Chu and Nieuwenhuijsen, 2002). According to the WHO, drinking water guidelines for the four THMs are 200 μg L^{-1} for chloroform, 60 μg L^{-1} for bromodichloromethane and 100 μg L^{-1} for both chlorodibromomethane and for bromoform (WHO, 1993).

Watts *et al.* (2007) studied the photodecomposition of chlorine species, such as NH_2Cl, $HOCl$, and OCl^-, on exposure to UV from LP and MP Hg lamps.
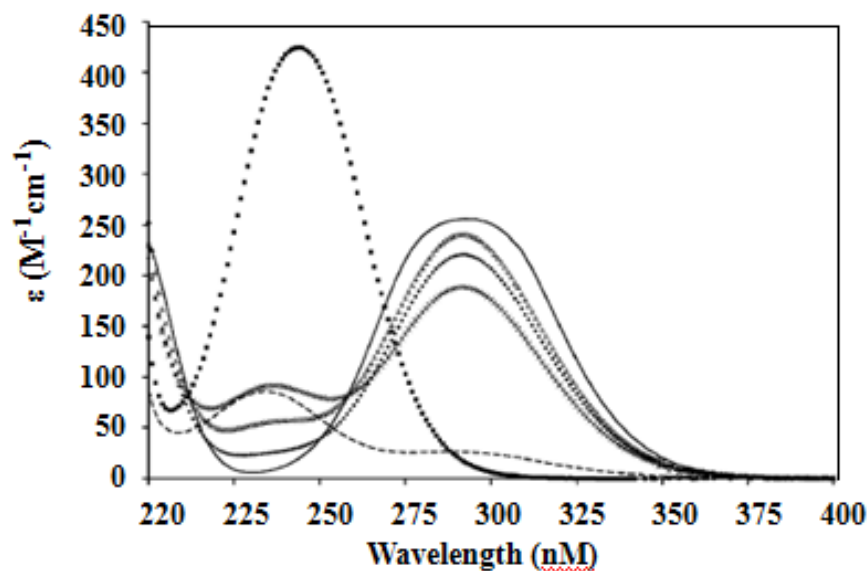
Figure 2.10 Molar absorption coefficients at each wavelength for NH_2Cl (■), OCl^- (——),
HOCl (– –), and active chlorine solutions at three pH values (Watts *et al.,* 2007)

From Figure 2.10, it can be concluded that monochloramine has the highest molar

absorption coefficient at 254 nm as compared to those of HOCl and OCl^-. However, the

comparison was made between the photodegradation quantum yields of active chlorine at

pH 7.1, 7.5 and 7.9 and HOCl, OCl^-, and NH_2Cl as shown in Figure 2.11. For active

chlorine at pH between 7 and 8, the observed Φ_{254} ranged from 1.3 to 1.7 mol/einstein;

Φ_{254} for HOCl was 1.5 mol/einstein. Whereas, the quantum yield for monochloramine at

254 nm varied from 0.3 to 0.7 mol/einstein between 200 and 300 nm. Thus, the

photodegradation of monochloramine was minimal in solutions exposed to either the LP

or MP UV sources (Watts *et al.,* 2007).
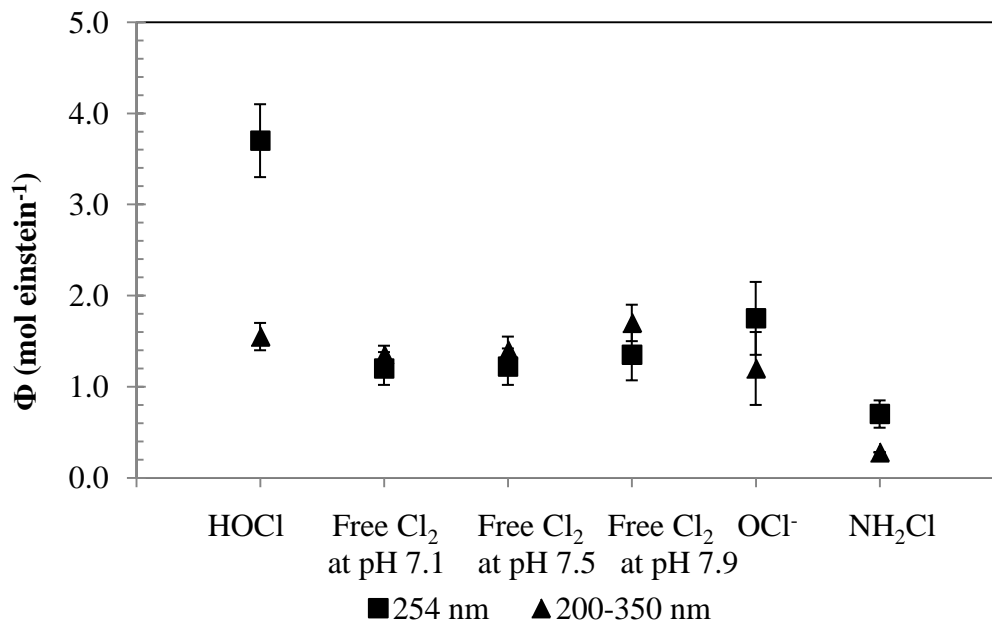
Figure 2.11 Photodegradation quantum yields at 254 nm (Δ) and at 200–350nm ($\blacksquare$) for the chlorine species: OCl^-, HOCl, active chlorine mixtures and NH_2Cl (Watts *et al.,* 2007)

This might indicate that the photodecomposition of monochloramine, which has the highest concentration among the combined chloramines, is negligible. Thus, in the case of swimming pools, there should be little concern for the photodecomposition of the combined chlorine species (i.e., the chloramines).

Cassan *et al.* (2006) investigated the effects of MP UV exposure on the water quality of swimming pools. In their study, they highlighted the additional formation of THMs, particularly $CHCl_3$ and $CHBrCl_2$, in the chlorinated water of an indoor swimming pool using a MP UV lamp for disinfection. However, during the experiment, the concentrations of $CHBr_3$ and $CHBr_2Cl$ decreased during the UV exposure. This might be explained as follows. First, the chlorinated water under UV exposure could form free radicals such as $\cdot OH$, $\cdot H$ and $\cdot Cl$ (Montiel, 1980), which could then break the carbon-hydrogen bond to form $CHCl_3$ from the organic matter in the water. These reactions have

very short lifetimes, and the products formed are very stable species having strong bond energies. The C–H bond energies of the THMs decrease in the order: $CHCl_3 > CHBrCl_2 > CHBr_2Cl > CHBr_3$, and this could explain the concentration decrease of $CHBr_3$ and $CHBr_2Cl$, since they have the weakest bonds in the family. Second, the increase of active chlorine by the photolysis of a part of combined chlorine may be the reason for the formation of chloroform. The study showed that when the chlorine injection is reduced, the $CHCl_3$ concentration was significantly reduced. Third, UV exposure might have increased the reactivity of organic materials (from the bathers in the swimming pool); this could lead to an additional source of THMs formation. Magnuson *et al.* (2002) reported that UV exposure from MP lamps could increase the reactivity of the natural organic matter toward chlorination.

Although there were extra THMs formed during the UV/Chlorine disinfection of the water in swimming pools, the concentrations of THMs were found to be lower than the regulatory limits. However, further studies on the effects of UV exposure on chlorinated waters have to be carried out to evaluate the overall process.

2.4   Summary

This chapter discusses mainly the fundamentals, possible applications, and some research achievements of chlorine photolysis when exposed to UV.

In Sections 2.1 and 2.2, the reactions and production of ·OH radicals under UV were discussed. The photolysis of active chlorine can depend on pH, the concentration of active chlorine, the presence of organic matter (TOC), temperature, and wavelength, etc.

As to the applications of the UV/Chlorine process, since it has an effective ability to produce ·OH radicals, it can be utilized as an Advanced Oxidation Processes in water/wastewater treatment. It might become an alternative technology in AOPs to the UV/H_2O_2 process. The UV/Chlorine process can also be used to validate the fluence delivered in UV reactors by utilizing the photodegradation behavior of active chlorine under UV.

As regards the impacts of the photochemical reactions of chlorine species on the UV disinfection system performance, the photodegradation of chlorine will result in some reduction of log removal during disinfection, although this reduction is not very significant. Furthermore, the photolysis of other chlorine species can impact the water quality of chlorinated swimming pools when the UV/Chlorine process is applied in swimming pool disinfection. Further studies on the effects of UV exposure of chlorinated water should be carried out to evaluate the specific processes involved.

2.5   References

Baxendale, J. H., and Wilson, J. A. (1957). "The Photolysis of Hydrogen Peroxide at High Light Intensities." Transactions of the Faraday Society, 53(3), 344-356.

Blatchley, E. R., and Hunt, B. A. (1994). "Bioassay for Full-Scale UV Disinfection Systems." Water Science and Technology, 30(4), 115-123.

Bolton, J.R. (2010) Ultraviolet applications handbook (3rd edition). ICC Lifelong Learn Inc., Edmonton, Canada.

Bolton, J.R. and Linden, K.G. (2003). "Standardized of methods for fluence (UV dose) determination in bench-scale UV experiments." Journal of Environmental Engineering 129 (3), 209–216.

Bolton, J. R., and Stefan, M. I. (2002). "Fundamental photochemical approach to the concepts of fluence (UV dose) and electrical energy efficiency in photochemical degradation reactions." Research on Chemical Intermediates, 28(7-9), 857-870.

Buxton, G. V., Greenstock, C. L., Helman, W. P., and Ross, A. B. (1988). "Critical-Review of Rate Constants for Reactions of Hydrated Electrons, Hydrogen-Atoms and Hydroxyl Radicals (.Oh/.O-) in Aqueous-Solution." Journal of Physical and Chemical Reference Data, 17(2), 513-886.

Buxton, G. V., and Subhani, M. S. (1972). "Radiation-Chemistry and Photochemistry of Oxychlorine Ions .1. Radiolysis of Aqueous-Solutions of Hypochlorite and Chlorite Ions." Journal of the Chemical Society-Faraday Transactions, 68, 947-956.

Cassan, D., Mercier, B., Castex, F., and Rambaud, A. (2006). "Effects of medium-pressure UV lamps radiation on water quality in a chlorinated indoor swimming pool." Chemosphere, 62(9), 1507-1513.

Chu, H., and Nieuwenhuijsen, M. J. (2002). "Distribution and determinants of trihalomethane concentrations in indoor swimming pools." Occup. Environ. Med., 59(4), 243-247.

Feng, Y., Smith, D. W., and Bolton, J. R. (2010). "A Potential New Method for Determination of the Fluence (UV Dose) Delivered in UV Reactors Involving the Photodegradation of Free Chlorine." Water Environ. Res., 82(4), 328-334.

Feng, Y., Smith, D. W., and Bolton, J. R. (2007). "Photolysis of aqueous free chlorine species (NOCI and OCI-) with 254 nm ultraviolet light." Journal of Environmental Engineering and Science, 6(3), 277-284.

Giles, M. A., and Danell, R. (1983). "Water Dechlorination by Activated Carbon, Ultraviolet-Radiation and Sodium-Sulfite - a Comparison of Treatment Systems Suitable for Fish Culture." Water Res., 17(6), 667-676.

Han, S. K., Nam, S. N., and Kang, J. W. (2002). "OH radical monitoring technologies for AOP advanced oxidation process." Water Science and Technology, 46(11-12), 7-12.

Hery, M., Hecht, G., Gerber, J. M., Gendre, J. C., Hubert, G., and Rebuffaud, J. (1995). "Exposure to Chloramines in the Atmosphere of Indoor Swimming Pools." Ann. Occup. Hyg., 39(4), 427-439.

Jin, S., Mofidi, A. A., and Linden, K. G. (2006). "Polychromatic UV fluence measurement using chemical actinometry, biodosimetry, and mathematical techniques." Journal of Environmental Engineering-ASCE, 132(8), 831-841.

Judd, S. J., and Jeffrey, J. A. (1995). "Trihalomethane Formation during Swimming Pool Water Disinfection using Hypobromous and Hypochlorous Acids." Water Res., 29(4), 1203-1206.

Kim, H., Shim, J., and Lee, S. (2002). "Formation of disinfection by-products in chlorinated swimming pool water." Chemosphere, 46(1), 123-130.

Linden, K. G., and Darby, J. L. (1997). "Estimating effective germicidal dose from medium pressure UV lamps." Journal of Environmental Engineering-Asce, 123(11), 1142-1149.

Magnuson, M. L., Kelty, C. A., Sharpless, C. M., Linden, K. G., Fromme, W., Metz, D. H., and Kashinkunti, R. (2002). "Effect of UV irradiation on organic matter extracted from treated Ohio River water studied through the use of electrospray mass spectrometry." Environ. Sci. Technol., 36(23), 5252-5260.

Mamane-Gravetz, H., and Linden, K. G. (2004). "UV disinfection of indigenous aerobic spores: implications for UV reactor validation in unfiltered waters." Water Res., 38(12), 2898-2906.

Massin, N., Bohadana, A. B., Wild, P., Hery, M., Toamain, J., and Hubert, G. (1998). "Respiratory symptoms and bronchial responsiveness in lifeguards exposed to nitrogen trichloride in indoor swimming pools." Occup. Environ. Med., 55(4), 258-263.

Montiel, A. J. (1980). *Les halométhanes dans l'eau, formation et elimination*, Imprimerie Bayeusaine, Bayeux.

Morris, J. C. (1966). "Acid Ionization Constant of HOCl from 5 to 35 Degrees." J. Phys. Chem., 70(12), 3798-3806.

Nash, T. (1953). "The colorimetric estimation of formaldehyde by means of the Hantzsch Reaction." J. Biochem., 55(3), 416-421.

Nieminski, E. C., Bellamy, W. D. and Moss, L.R. (2000). "Using surrogates to improve treatment plant performance." Journal of the American Water Works Association. 92(3), 67-78.

Nowell, L. H., and Hoigne, J. (1992a). "Photolysis of Aqueous Chlorine at Sunlight and Ultraviolet Wavelengths .1. Degradation Rates." Water Res., 26(5), 593-598.

Nowell, L. H., and Hoigne, J. (1992b). "Photolysis of Aqueous Chlorine at Sunlight and Ultraviolet Wavelengths .2. Hydroxyl Radical Production." Water Res., 26(5), 599-605.

Oliver, B. G., and Carey, J. H. (1977). "Photochemical Production of Chlorinated Organics in Aqueous-Solutions Containing Chlorine." Environ. Sci. Technol., 11(9), 893-895.

Örmeci, B., Ducoste, J. J., and Linden, K. G. (2005). "UV disinfection of chlorinated water: impact on chlorine concentration and UV dose delivery." Journal of Water Supply Research and Technology-Aqua, 54(3), 189-199.

Quan, Y., Pehkonen, S. O., and Ray, M. B. (2004). "Evaluation of three different lamp emission models using novel application of potassium ferrioxalate actinometry." Ind. Eng. Chem. Res., 43(4), 948-955.

Rahn, R. O., Stefan, M. I., Bolton, J. R., Goren, E., Shaw, P. S., and Lykke, K. R. (2003). "Quantum yield of the iodide-iodate chemical actinometer: Dependence on wavelength and concentration." Photochem..Photobiol., 78(2), 146-152.

Thomsen, C. L., Madsen, D., Poulsen, J. A., Thogersen, J., Jensen, S. J. K., and Keiding, S. R. (2001). "Femtosecond photolysis of aqueous HOCl." J..Chem..Phys., 115(20), 9361-9369.

USEPA. (2006). "Ultraviolet disinfection guidance manual for the final long term 2 enhanced surface water treatment rule, EPA 815-R-06-007". 1200 Pennsylvania Avenue NW Washington

Wait, I. W. (2008). "Multiple-Barrier Disinfection by Chlorination and UV Irradiation for Desalinated Drinking Waters: Chlorine Photolysis and Accelerated Lamp-Sleeve Fouling Effects." Water Environ. Res., 80(11), 2183-2188.

Watts, M. J., and Linden, K. G. (2007). "Chlorine photolysis and subsequent OH radical production during UV treatment of chlorinated water." Water Res., 41(13), 2871-2878.

World Health Organization (WHO). (1993). *Guidelines for Drinking Water*. Geneva, Switzerland.

Zepp, R.G. (1982). *The Handbook of Environmental Chemistry*. Springer, Berlin.

Zheng, M. S., Andrews, A. and Bolton, J. R. (1999) "Impacts of medium-pressure UV and UV/H_2O_2 treatments on disinfection by-product formation." *Proc., AWWA 1999 Annual Conference*. Chicago, IL.

CHAPTER 3 INVESTIGATION OF THE UV/CHLORINE PROCESS IN THE PRESENCE OF METHANOL

3.1 Introduction

As discussed in Chapter 1, the principle purpose of this research is to investigate the potential of the UV/Chlorine process in producing ·OH radicals, which can then act to remove organic contaminants in water/waste waters.

Feng *et al.,* (2007) observed the formation of formaldehyde when methanol was added into a hypochlorous acid solution exposed to UV. In this Chapter, the production of formaldehyde and the appropriate photodegradation quantum yields using the UV/Chlorine process in the presence of methanol are quantified and compared to those of the UV/H_2O_2 process. To fulfill this purpose, the following experiments were designed and performed:

1. Examine the photolysis of chlorine species in water (HOCl at pH 5 and OCl$^-$ at pH 10) in regard to the generation of hydroxyl radicals (·OH).

2. Measure the quantum yields for the generation of ·OH radicals in the UV/Chlorine process in the presence of methanol by measuring the production of formaldehyde at pH 5 and 10.

3. Measure the quantum yields for the generation of ·OH radicals in the UV/H_2O_2 process in the presence of methanol by measuring the production of formaldehyde.

4.   Compare the degradation efficiency of methanol between the UV/Chlorine

process and other Advanced Oxidation Processes (e.g., the UV/H$_2$O$_2$ process).

3.2   Materials and Methods

3.2.1   Materials and equipment

Analytical reagent grade chemicals were used for the preparation of all the samples.

MilliQ water was generated by a Maxima Ultra Pure Water System, and was used for

preparation of solutions. Chlorine samples were prepared using a 10%−15% sodium

hypochlorite solution obtained from Sigma-Aldrich[®], and the concentration of active

chlorine was measured by the DPD total chlorine reagent for 5 mL samples (Hach[®],

Anachemia Canada Inc.). Hydrogen peroxide samples were prepared using a 30%

hydrogen peroxide solution from Fisher Scientific[®]. Excess H$_2$O$_2$ was removed by using

catalase (oxidoreducatase obtained from Sigma[®]), and the remaining catalase was filtered

from the solutions using a 0.2 μm nylon syringe filter (purchased from Whatman[®]).

HPLC grade methanol was also purchased from Fisher Scientific[®].

A quasi collimated beam UV apparatus (Model PSI-I-120, Calgon Carbon Corporation,

USA) equipped with a low pressure high output (LPHO) UV lamp (LSI Inc.) was used to

generate quasi-parallel UV with a wavelength of 254 nm. The irradiance in the UV

collimated beam was measured by a UV detector (International Light, Model SED240)

connected to a radiometer (International Light, Model IL 1400A).

The pH of aqueous samples was measured by a pH meter (Accumet® Research AR50, Fisher Scientific Co., Canada) using a magnetic stirrer (Isotemp®, Fisher Scientific Co., Canada).

For absorption measurements of aqueous chlorine solutions, an Ultraspec 2000 UV-Visible spectrophotometer (Pharmacia Biotech, fisher Scientific Co., Canada) and 10.0 mm path length quartz cells (Fisher Scientific Co., Canada) were used.

3.2.2   Preparation of samples

3.2.2.1 Preparation of chlorine samples

Chlorine samples were prepared freshly for each trial by adding 10%–15% sodium hypochlorite (Fisher Scientific Co., Canada) into MilliQ water based on the concentration of chlorine sample to be used.

After adding the desired amount of sodium hypochlorite solution, buffer solutions were also prepared to obtain pH 5 and 10 for chlorine samples. The amount of chemical reagents for each buffer was calculated from the acid-base chemistry as follows:

$$[3.1]\quad HA \leftrightarrow H^+ + A^-$$

$$[3.2]\quad K_a = [H^+][A^-]/[HA]$$

where K_a is the acid dissociation constant of HA.

$$[3.3]\quad [HA] + [A^-] = C$$

where C is the concentration of the buffer solution.

[3.4] $\dfrac{[A^-]}{[HA]} = 10^{\text{pH}-\text{p}K_a}$

where $\text{p}K_a = -\log(K_a)$, and pH is the desired pH value of the buffer solution.

By combining equations 3.3 and 3.4, the quantity of the chemicals that needs to be added to the solution can be calculated.

Feng *et al.,* (2007) investigated the buffer effect on the photodegradation quantum yields of active chlorine and indicated that buffer concentrations from 20 to 120 mM had no significant effect on the quantum yields. In this research, concentration of the buffer solution was 10 mM. Table 2.1 shows the chemical reagents used for preparation of buffer solutions for pH 5 and 10. The concentrations of the buffer were 10 mM for both the pH 5 and pH 10 solutions.

Table 2-1 Chemical reagents used for the preparation of buffer solutions

Desired pH	Chemicals added		$\text{p}K_a$
	HA	A-	
5	CH_3COOH	CH_3COONa	4.74
10	$NaHCO_3$	Na_2CO_3	10.33

3.2.2.2 Preparation of hydrogen peroxide samples

The preparation of hydrogen peroxide solutions was similar to that of the chlorine samples, namely by adding a calculated amount of a 30% H_2O_2 solution into a 1 L volumetric flask containing MilliQ water.

3.2.2.3 Preparation of samples containing methanol

Samples containing methanol were prepared by adding certain volume of methanol, taking account of the density of methanol, into the target solutions to obtain the desired concentration of methanol.

3.2.3　Sample measurements

3.2.3.1 Chlorine concentration measurements

In this study, the DPD colorimetric method was adopted, since the chlorine concentration in the samples was usually less than 50 mg/L according to the *Standard Methods for the Examination of Water and Wastewater* (APHA *et al.,* 1995b).

DPD powder (for 5 mL sample, Hach®, Anachemia Science co.) was added into chlorine samples, and the absorbance at 515 nm of the product was measured using a spectrophotometer. This method is applicable for chlorine concentration ranging from 10 μg/L – 50 mg/L.

Brief procedures to the determination of chlorine concentration:

1. A standard curve was prepared as follows:

    a. A series of potassium permanganate standard solutions was prepared (0.891 mg/L potassium permanganate solution corresponds to 1.0 mg/L active chlorine), the concentrations of which corresponded to 0.5, 1.0, 2.0, 3.0, and 4.0 mg/L active chlorine;

    b. Transfer 5 mL of each standard solution into 10 mL beakers, adding a pouch of DPD active chlorine powder; stir the sample on a magnetic stirrer

c. Measure the absorbance of each sample at 515 nm;

d. Plot the absorbance corresponding to each chlorine concentration and obtain the standard curve for chlorine concentration (Figure 3.1 gives a typical example).
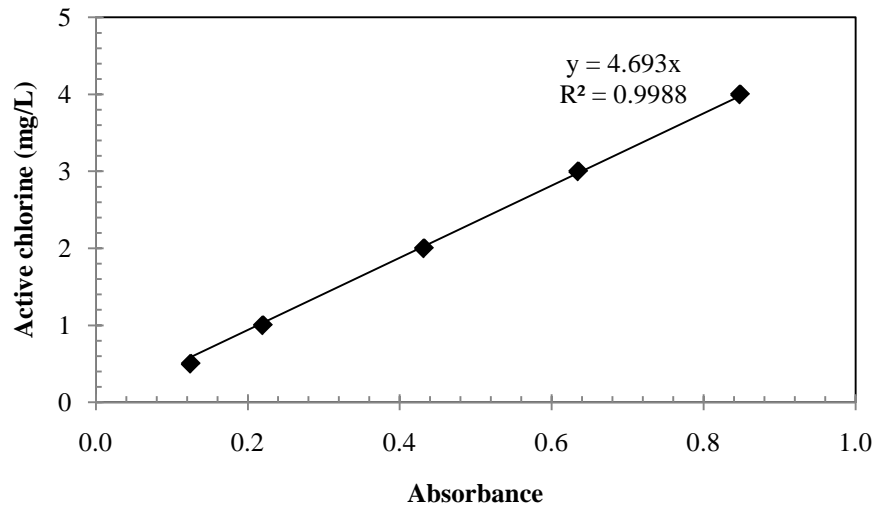
Figure 3.1 Standard curve for the active chlorine concentration using the DPD colorimetric method

2. A 5 mL aliquot of the sample was transferred to a 10 mL vial;

3. A pouch of DPD powder was added to the vial;

4. After sufficient mixing, the absorbance of the solution was measured at 515 nm using a spectrophotometer;

5. The active chlorine concentration was measured and calculated by the standard curve obtained in step 1.

3.2.3.2 Determination of hydrogen peroxide concentration

The concentration of hydrogen peroxide was determined by measuring the absorbance at the optical wavelength: 240 nm, where $\varepsilon_{240} = 38.1 \ M^{-1} \ cm^{-1}$ (Goldstein *et al.*, 2007).

3.2.3.3 Determination of the formaldehyde concentration

The amount of formaldehyde produced after photolysis of UV/Chlorine or UV/H$_2$O$_2$ solutions was measured by the method developed by Nash (1953). A reagent that contained 2 M or approximately 150 g ammonium acetate, 0.05 M acetic acid and 0.02 M acetyl acetone was prepared. This reagent was mixed with an equal volume of sample to be tested, and the mixed sample was incubated in an oven for 5 min at 60 °C. After the incubation and cooling of the sample, the absorbance of the incubated sample at the wavelength of 412 nm was measured. The molar absorption coefficient (ε_{412}) of the mixture at 412 nm is 7,700 mol^{-1} cm^{-1} (Nash, 1953). Thus, the concentration of formaldehyde can be calculated by the absorbance and ε_{412}. The method is valid for formaldehyde concentrations up to 8 mg/L. Since there was control sample for each run, the formaldehyde produced in the control sample was also measured.

3.2.4 UV collimated beam exposure and calibration of the radiometer

For each run under the UV collimated beam, two 20 mL beakers of active chlorine or hydrogen peroxide samples were prepared, one of which was exposed to UV, and the other was kept in the dark as a control experiment. A 3 mm × 12 mm Teflon™-coated stir bar was added into each sample to be treated under the UV collimated beam, and the beaker was put on a magnetic stirrer (Isotemp®, Fisher Scientific Co., Canada), so that the sample could be thoroughly mixed during the exposure. The height from the lamp position to the sample could be adjusted to obtain the proper irradiance.

Before each run, an appropriate exposure time was set to the stopwatch that controls the pneumatic shutter located beneath the UV lamp and at the top of the collimating tube.

The irradiance of the collimated beam was measured by placing a radiometer with a UV

detector (International Light, Model SED240) right under the center of the collimated

beam by adjusting the calibration marker of the detector to a height that was the same as

the top of the solution when placed under the collimated beam. A diagram of the UV

collimated beam apparatus is shown in Fig. 3.2.
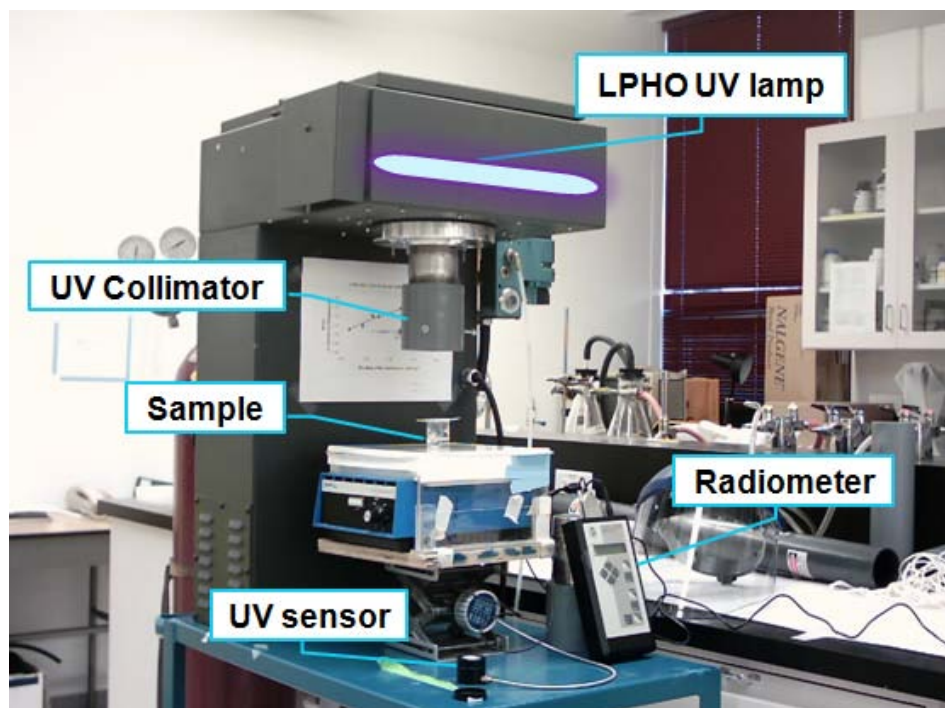
Figure 3.2 Diagram of the UV Collimated beam apparatus

Furthermore, a calibration of the radiometer was necessary before measuring the

irradiance of the LP UV lamp. The radiometer was calibrated by the KI/KIO_3 actinometer

method (Bolton et al, 2009). The irradiance, as determined in the calibration procedure,

was found to be essentially the same as that given on the readout of the radiometer.

3.2.5 UV/Chlorine process procedures

Before the experiments, a chlorine solution buffered to the desired pH was prepared according to Section 3.2.2, and the glassware was cleaned for use. The trials were conducted according to the steps as follows:

1. Measure the chlorine concentration and the pH of the sample solution prior to the trials.

2. Turn on the UV lamp on the collimated beam apparatus and let the irradiance stabilize for at least 15 min before each trial, and set the desired exposure time on the timer.

3. Prepare the samples for the trial while the lamp is warming up. Transfer 20 mL aliquots of the sample solution to both sample and control vials and add a 3 mm × 12 mm Teflon™-coated stir bar to each vial.

4. When the lamp is warmed up, open the shutter of the collimated beam and put the radiometer UV detector under the UV beam. Measure the irradiance using the radiometer connected to the UV detector. Make sure that the calibration marker of the detector is as the same distance from the lamp position as that of the top of the solution when the sample is placed underneath the collimated beam.

5. Remove the UV detector after the irradiance has been measured. Put the test vial under the UV collimated beam on a magnetic stirrer and adjust the position of the vial to the center of the projective area beneath the collimating tube. Measure the distance from the lamp position to the top of solution.

6. Begin the trial by turning on the pneumatic shutter button and turn on the magnetic stirrer so that the sample is adequately mixed all through the trial. Keep the control sample in the dark.

7. After the trial, the pneumatic shutter closes automatically to block off the UV. Then remove the sample from the stirrer.

8. Measure the chlorine concentration and formaldehyde production in both the test and the control samples.

9. Other photolysis experiments were also carried out according to the steps above.

3.3   Results and discussion

3.3.1   Photodegradation quantum yield of active chlorine at pH 5

As an essential experiment in the literature of the UV/Chlorine process, the photodegradation quantum yield of active chlorine was investigated again in this research.

The study began with repeating some trials from previous studies. The photodegradation quantum yields of active chlorine at pH 5, which are known to be approximately 1.0 (Feng *et al.*, 2007), were repeated to determine whether the proper design and procedures of the experiments had been achieved.

The UV/Chlorine process trials were carried out using increasing chlorine concentration up to 90 mg/L. As the chlorine dose increased, the fluence (UV dose) was also set larger accordingly to obtain proper removal of the chlorine. The photodegradation quantum yields were calculated from Eqs. (2.3), (2.4) and (2.5). The results (see Figure 3.3) show that photodegradation quantum yield of active chlorine at pH 5 is essentially constant at 1.03 ± 0.11 when the concentration is less than 90 mg/L.
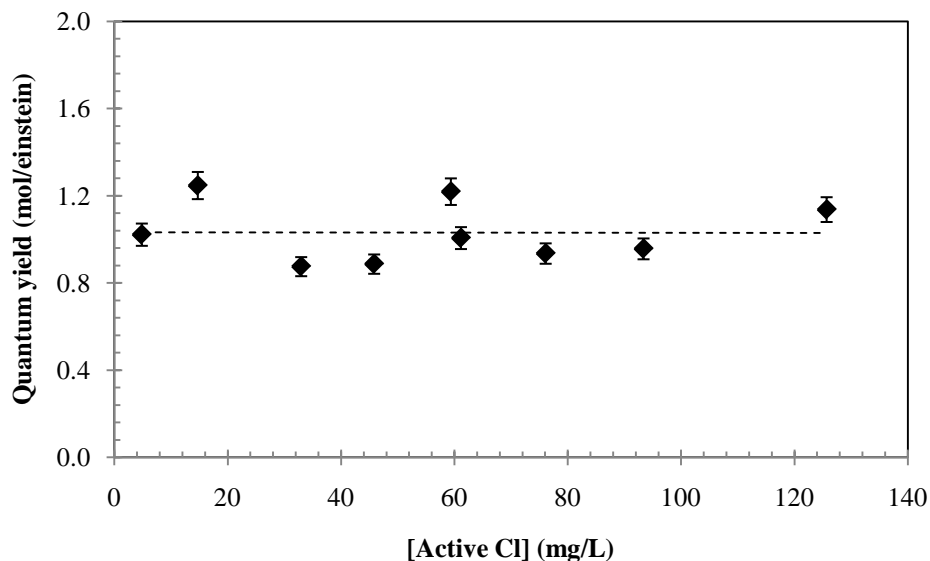
Figure 3.3 Photodegradation quantum yields of active chlorine (Cl) at pH 5 and temperature $20 \pm 2\ ^{o}C$

3.3.2 Photodegradation quantum yield of active chlorine in the presence of methanol at pH 5 and 10

As discussed above, the photodegradation quantum yield of active chlorine measured in MilliQ water was around 1.0. However, due to the presence of NOMs in natural waters, there are various kinds of organic compounds that can become radical scavengers and cause chain reactions in the UV/Chlorine process and hence lead to further consumption of HOCl, as studied by Oliver and Carey (1970).They carried out a series of experiments around pH 4 using radical scavengers, such as ethanol, n-butanol and benzoic acid and proposed the following chain reactions:
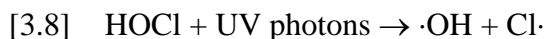
[3.8] $HOCl + UV\ photons \rightarrow \cdot OH + Cl\cdot$

$\cdot OH$ radical chain reactions:

[3.9] $\cdot OH + RH \rightarrow \cdot R + H_2O$

[3.10] $\cdot R + HOCl \rightarrow RCl + \cdot OH$

$\cdot Cl$ radical chain reactions:

[3.11] $\cdot Cl + RH \rightarrow \cdot R + HCl$

[3.12] $\cdot R\ \ + HOCl \rightarrow ROH + \cdot Cl$

When methanol was introduced to the samples at pH 5, where HOCl mainly exists, there occur chain reactions and oxidative reactions as follows:

[3.6] $\cdot OH + CH_3OH \rightarrow \cdot CH_2OH + H_2O$

[3.7] $\cdot CH_2OH + HOCl \rightarrow ClCH_2OH + \cdot OH$

[3.8] $\cdot CH_2OH + O_2 \rightarrow \cdot O_2CH_2OH \rightarrow HCHO + HO_2\cdot$

The production of formaldehyde can be detected and quantified by the Nash method (Nash, 1953). Since the efficiency of $\cdot OH$ radicals reacting with methanol in reaction [3.6] is 93% (Asmus *et al.,* 1973), the $\cdot OH$ radicals production can be calculated by the amount of formaldehyde produced.

Knowing that methanol can increase the photodegradation quantum yield of active chlorine at pH 5, methanol was selected to be the first 'challenge' scavenger in order to analyze the oxidation reactions in the UV/Chlorine and UV/H$_2$O$_2$ processes. Samples with various methanol concentrations were prepared to investigate the competition kinetics of methanol reacting with $\cdot OH$ radicals. A relation between methanol concentration and formaldehyde production showed a plateau region indicating the methanol concentration around which methanol becomes the principal radical scavenger.

Also the photodegradation quantum yield for active chlorine and that of the ·OH radical production were determined.

Samples containing 9.9 – 86.5 mM methanol and approximately 50 mg/L active chlorine at pH 5 were prepared. Each sample was exposed to UV in a collimated beam apparatus for 300 s with a LP UV lamp and the irradiance 0.38 mW/cm^2. According to Feng *et al.,* (2007), the production of formaldehyde was detected after the UV/Chlorine process in the presence of methanol. The formaldehyde concentration was quantified according to the procedure given in Section 3.2.3.3. The chlorine concentrations were measured according to Section 3.2.3.1.

Figure 3.4 shows that the photodegradation quantum yield for 50 mg/L active chlorine at pH 5 does depend on the concentration of methanol. From the figure, the quantum yield increased from 1.0 up to 16.6 mol einstein^{-1} when the methanol concentration increased from 0.0 to 86.5 mM.
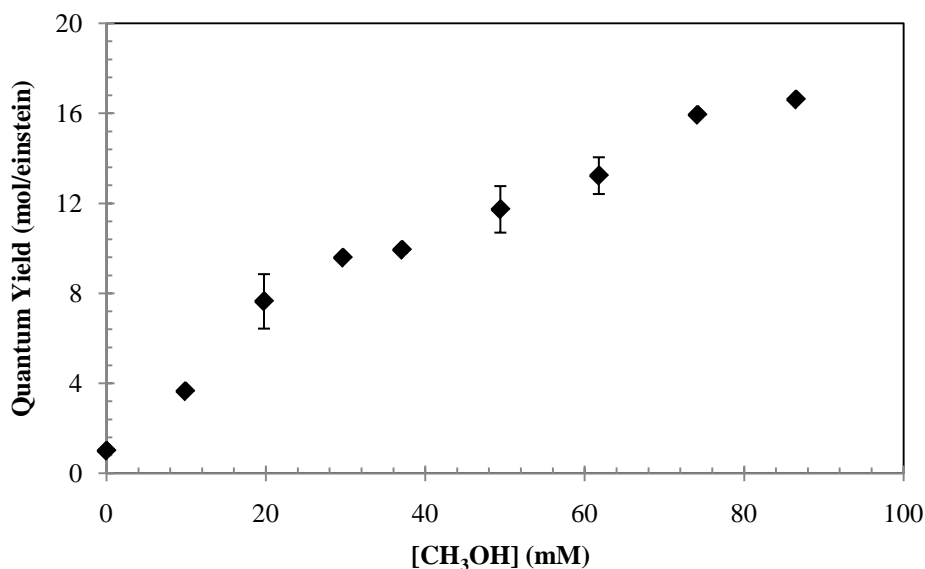
Figure 3.4 Photodegradation quantum yield of active chlorine (50 mg/L) at pH 5.0 in the presence of various concentrations of methanol (mM)

Feng *et al.,* (2007) conducted similar experiments, and the quantum yields obtained in his research were larger than the quantum yields obtained in this research at the same methanol doses. The reason is the difference of the initial chlorine concentrations: the initial active chlorine concentration was 6 mM in his research, which is much higher than that in this research as presented above (1.33 mM). Feng *et al.,* (2007) proved that higher chlorine concentrations could result in higher quantum yields in the presence of methanol.

Samples containing approximately 50 mg/L free chlorine at pH 10 and various concentrations of methanol ranging from 9.9 – 61.8 mM were also prepared and exposed under the same LP UV lamp (the irradiance of which was 0.38 mW/cm^2) in a collimated beam apparatus for 600 s. The chlorine concentrations were measured according to Section 3.2.3.1, and photodegradation quantum yields for the trials were calculated and graphed as shown in Figure 3.5.
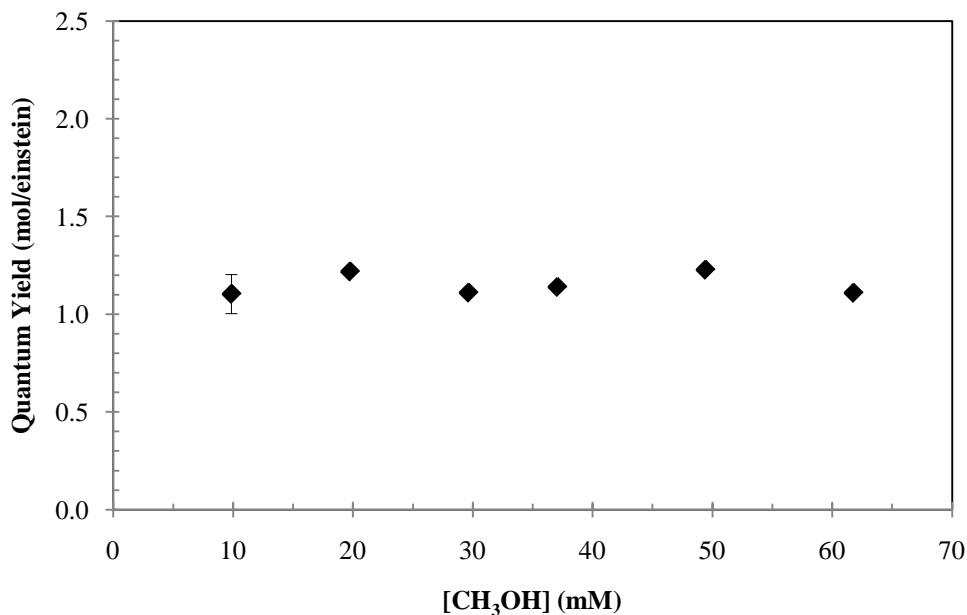

Figure 3.5 Photodegradation quantum yield of active chlorine at pH 10 in the presence of various methanol doses (mM)

As shown in Figure 3.5, the photodegradation quantum yields for chlorine samples at pH 10 did not show the increasing trend as in that of Figure 3.3. On the contrary, the quantum yields remained 1.15 ± 0.08 mol einstein^{-1}, indicating that the quantum yields of active chlorine at pH 10 do not depend on the methanol dose.

3.3.3 Quantum yield of the production of ·OH radicals in the UV/H$_2$O$_2$ process in the presence of methanol

The efficiency in oxidizing methanol and the production rate of ·OH radicals were compared between the UV/Chlorine and the UV/H$_2$O$_2$ processes, where similar experiments using methanol as a challenging radical scavenger were carried out using the UV/H$_2$O$_2$ process.

Previous studies have shown the quantum yield [Φ(·OH)] for the photodegradation of hydrogen peroxide in solutions exposed to UV has a quantum yield of about 1.0 (Legrini *et al,*. 1993) (without the introduction of organic compounds). The theoretical quantum yield of ·OH radical production should be 2.0. However, due to a cage reaction, during which two ·OH radicals combine with each other to form H$_2$O$_2$ molecules again, the actual quantum yield is much lower. Theoretically, the photodegradation quantum yields of H$_2$O$_2$ solutions in the presence of methanol should still be around 1.0, since the photodecomposition of H$_2$O$_2$ presumably cannot trigger chains reactions that can increase the quantum yield. In this study, experiments were carried out to verify that the quantum yields of hydrogen peroxide generating ·OH radicals are around 1.0.

Samples containing 151.7 mg/L H$_2$O$_2$ with methanol concentration varying from $1.0 -$ 49.3 mM were prepared and exposed to LP UV at an irradiance of 0.38 mW/cm^2 in a

collimated beam apparatus for 2700 s. The H_2O_2 concentrations were measured by the method described in Section 3.2.3.2.

Unlike the increasing quantum yields $[\Phi(\cdot OH)]$ in the UV/Chlorine process with increasing methanol concentration, the photodegradation quantum yields of for the UV/H_2O_2 process remained almost the same regardless of the addition of methanol. Figure 3.6 shows the H_2O_2 photodegradation quantum yields in the UV/H_2O_2 process with increasing methanol concentrations.
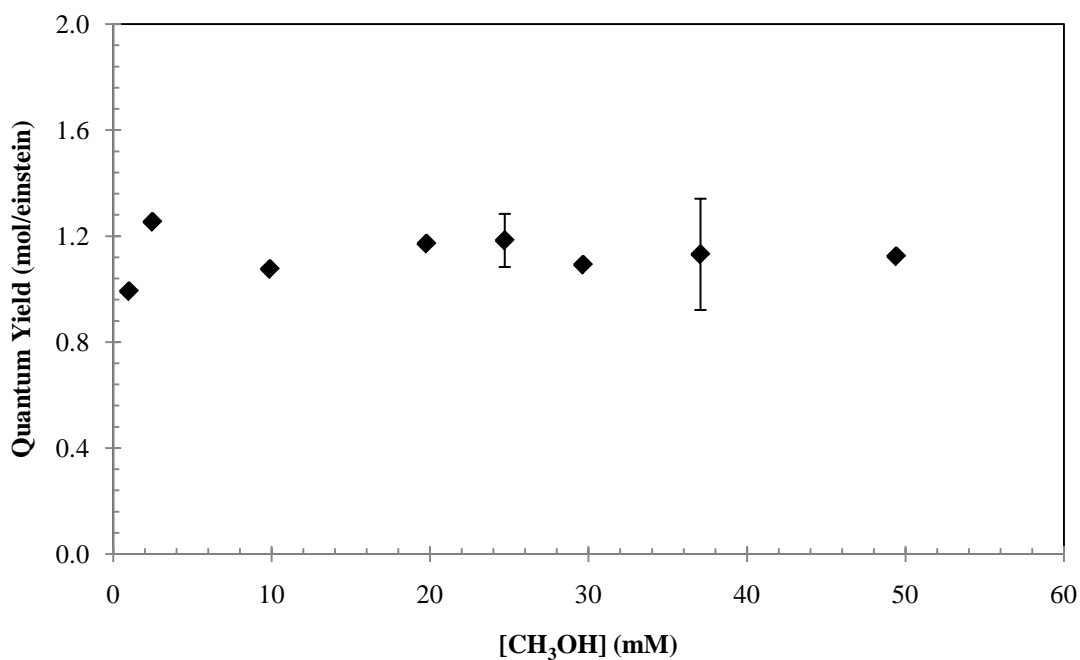
Figure 3.6 Photodegradation quantum yield of H_2O_2 (151.7 mg/L) in the presence of various methanol concentrations (mM)

As shown in Figure 3.6, the quantum yields $[\Phi(\cdot OH)]$ of hydrogen peroxide stayed in the range of 1.12 ± 0.13 mol einstein^{-1}, indicating that the increase of methanol does not stimulate an increase in the photodegradation quantum yields of the UV/H_2O_2 process.

3.3.4 Generation of ·OH radicals in the UV/Chlorine process

To investigate the oxidation efficiency of the UV/Chlorine process as an AOP, the generation of ·OH radicals was calculated from the production of formaldehyde during the UV/Chlorine process in the presence of methanol.

For the samples containing 9.9 – 61.8 mM methanol and approximately 50 mg/L active chlorine at pH 5, which were discussed in Section 3.3.2, the residual chlorine was quenched by adding 50 μL of 20 g/L sodium thiosulphate, and the formaldehyde concentration was measured as Section in 3.2.3.3. The relation between the production of formaldehyde (mM) and the addition of methanol (mM) is shown in Figure 3.7.
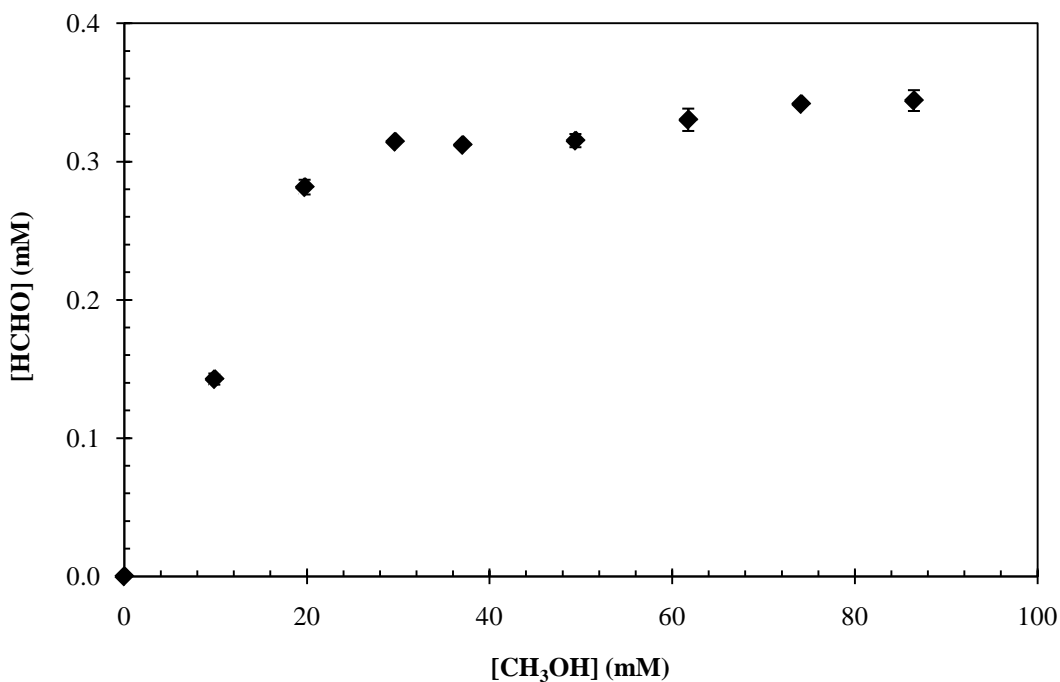
Figure 3.7 Production of formaldehyde as a function of the methanol concentration (mM) in the UV/Chlorine process at pH 5 showing a plateau region.

Figure 3.7 shows formaldehyde concentration increased as the methanol concentration increased. When the methanol concentration rises to about 25 mM, the formaldehyde

production becomes almost constant. At lower methanol concentrations, since methanol/chlorine ratio is lower, the competition of active chlorine with methanol over ·OH radicals at such conditions decreases the production of formaldehyde. At high methanol concentrations, methanol becomes the dominant radical scavenger and thus the production of formaldehyde becomes constant and independent of the methanol concentration.
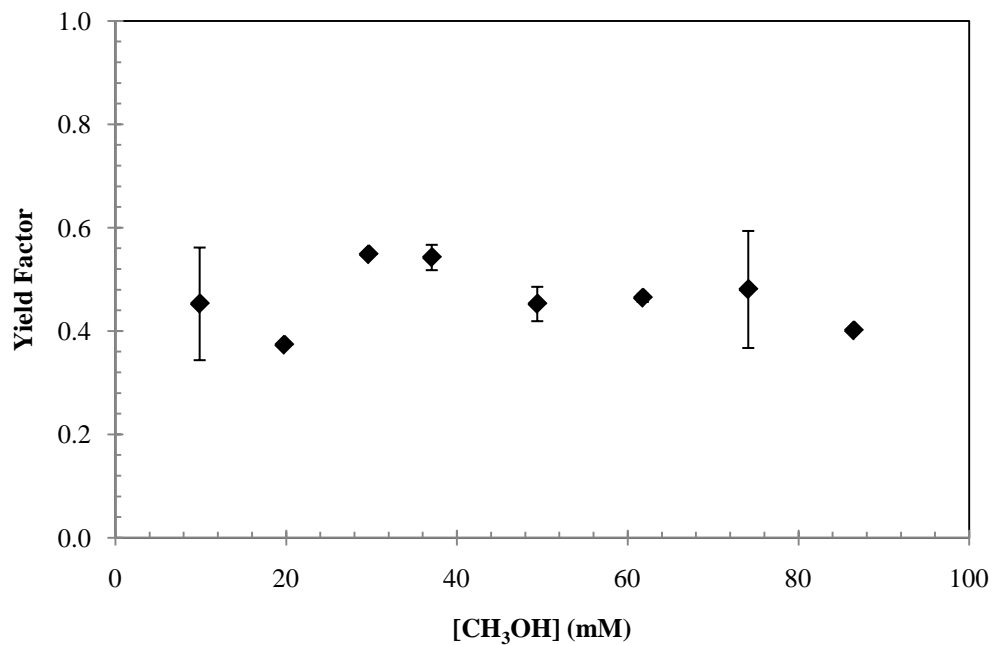
Figure 3.8 The ·OH radical production yield factors for various methanol doses (mM) in the UV/Chlorine process at pH 5.

Figure 3.8 shows the yield factors for the production of ·OH radicals in the samples described in the earlier part of this section. The figure shows that there was almost no increase in the yield factor, since the slope of the regression line was almost zero. The yield factors stayed around 0.46 ± 0.09, which were much smaller than 1.0.

The first-order fluence-based rate constant k_1' for each methanol concentration can be calculated according to Eq. (2.7). Further experiments were carried out with methanol concentrations varying from 9.9 to 86.5 mM and with the chlorine concentrations still at 1.33 mM at pH 5.
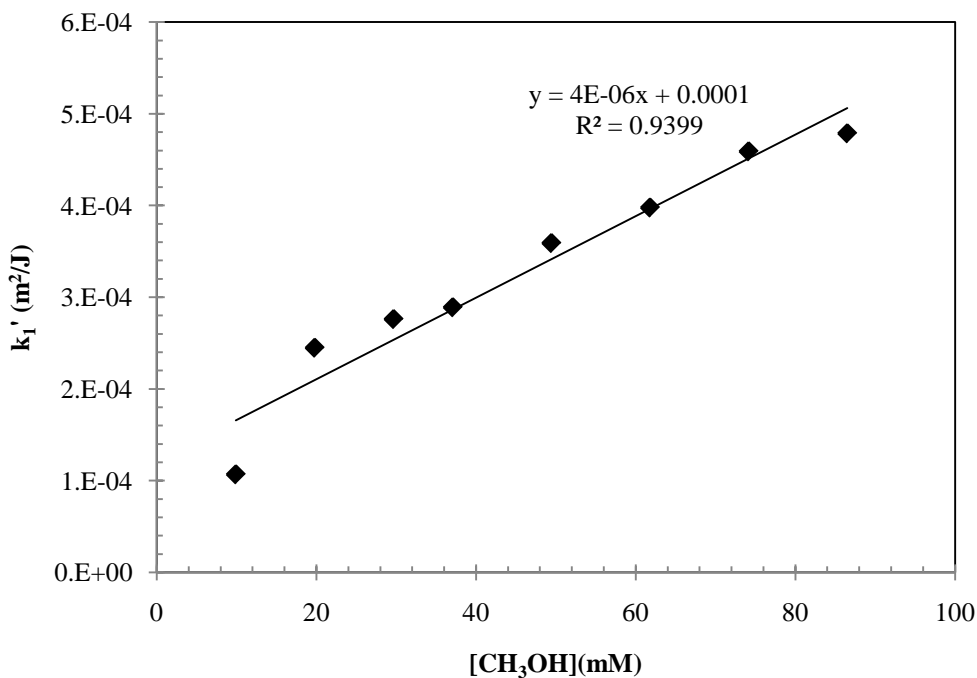
Figure 3.9 First-order fluence based rate constants k_1' for various doses of methanol (mM)

Figure 3.9 shows that k_1' also increases as the methanol concentration increases.

3.3.5 Generation of ·OH radicals in the UV/H_2O_2 process

The production of ·OH radicals was also calculated by measuring the production of formaldehyde after the H_2O_2 solutions are exposed to the LP UV. The formaldehyde concentrations were measured after the samples (containing 151.7 mg/L H_2O_2 with the methanol concentration varying from 1.0 – 49.3 mM) had been exposed under the UV collimated beam apparatus for 2700 s. The residual hydrogen peroxide was quenched

using catalase (Sigma[®]), and the samples were filtered before the concentrations of formaldehyde were measured.

As shown in Figure 3.10, the relation between formaldehyde production and methanol concentration formed a plateau region at a methanol dose of approximately 25 mM, showing the concentration of methanol around which methanol becomes the dominant radical scavenger, similar to the results obtained in the UV/Chlorine process in the presence of methanol.
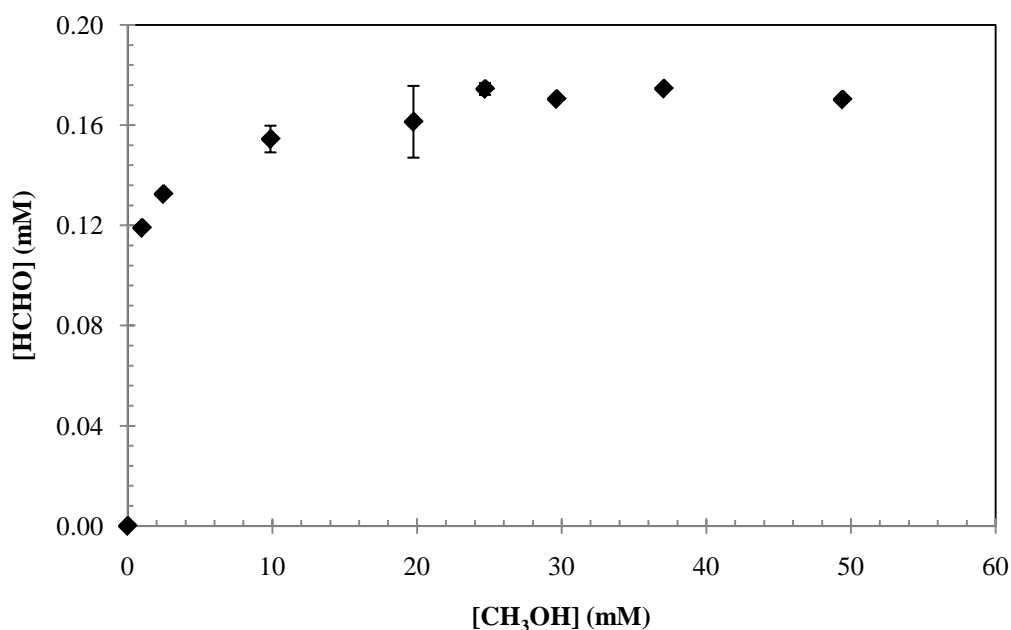
Figure 3.10 Plateau for methanol concentration (mM) and production of formaldehyde concentration (mM) in the UV/H$_2$O$_2$ process.

The yield factors (η) for the samples were calculated by ratio of the ·OH produced and the H$_2$O$_2$ decomposed during the photolysis according to Eq. (2.2), and are shown in Figure 3.11.

It should be mentioned that at low methanol doses, such as 1 and 2.5 mM methanol, although the formaldehyde production had already reached about 0.13 mM and began to become stabilized, a considerable consumption of hydrogen peroxide was observed. As a result, the yield factors at low methanol doses were much smaller than 1.0 and close to 0.
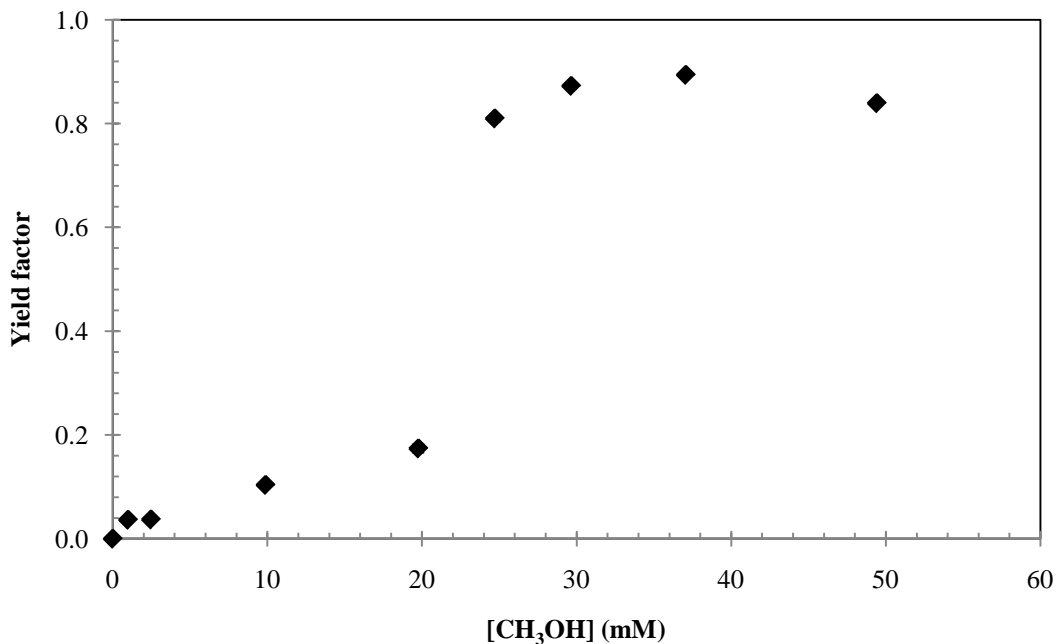
Figure 3.11 The yield factors for the UV/H$_2$O$_2$ process in the presence of various methanol concentration (mM).

It could be observed from Figure 3.10 that the yield factor increased as more methanol was introduced to the sample solutions. When the methanol concentration reached around 25 mM, the yield factor became stable around 0.85 ± 0.04.

3.4 Conclusions

This study began by repeating the photodegradation quantum yields of active chlorine around pH 5 and achieved similar results showing that the photodegradation quantum

yields were around 1.0 ± 0.1 when the chlorine concentration is under 90 mg/L as similar results shown in previous studies (Feng *et al.,* 2007).

Having obtained proper experimental designs and procedures and discussed the main reactions happening between ·OH and methanol, the study investigated the photodegradation quantum yields of active chlorine at both pH 5 and 10 in the presence of various methanol concentrations. Furthermore, the production from the photolysis process was also studied and quantified. Parallel experiments were also conducted for the UV/H$_2$O$_2$ process to compare the two processes.

The results show that photodegradation quantum yields of active chlorine at pH 5 no longer stay around 1.0 when the methanol was added into the samples. As the methanol doses increased from 9.9 – 61.8 mM, then quantum yields increased from 3.6 up to 21.1 mol einstein^{-1} which indicates that the addition of methanol did trigger chain reactions in the UV/Chlorine process by increasing the quantum yields to a larger scale. On contrary, the photodegradation quantum yields of active chlorine at pH 10 did not increase with the addition of methanol and remained around 1.15 ± 0.08 mol einstein^{-1}, which indicates that the chlorine photolysis at pH 10 was not affected by the addition of organic compounds.

Furthermore, at pH 5 the formaldehyde (produced from methanol being oxidized in the UV/Chlorine process) production increased as the methanol doses increased, while around a methanol concentration 25 mM, the formaldehyde production tended to become constant by forming a plateau area. This very fact indicates that as methanol dose increased to a certain point, methanol becomes the dominant radical scavenger.

Interesting results were obtained in the case of the UV/H$_2$O$_2$ process in the presence of various methanol doses. Similar to those of the UV/Chlorine process at pH 10, the photodegradation quantum yields remained around 1.0. However, the process did show the production of formaldehyde forming a plateau area as the methanol doses increased. It can be concluded that the competition for ·OH radicals also occurred during this process, while the production of ·OH radicals cannot be stimulated by methanol since the quantum yields did not increase and still stayed around 1.0.

The results from the addition of methanol in both the UV/Chlorine and the UV/H$_2$O$_2$ processes showed that the former can be stimulated by methanol and produce more ·OH radicals, and that the methanol dose can reach a certain point in order to become the main competitor for the ·OH radicals.

3.5   References

APHA. (1995). *Standard Methods for the Examination of Water and Wastewater (19th ed.),* American Public Health Association/American Water Works Association/Water Environment Federation, Washington, DC, USA.

Asmus, K. D., Mockel, H., and Henglein, A. (1973). "Pulse Radiolytic Study of Site of Oh Radical Attack on Aliphatic Alcohols in Aqueous-Solution." J. Phys. Chem., 77(10), 1218-1221.

Bolton, J. R., Stefanmn, M. I., Shaw, P. S. and Lykke, K. R. (2009). "Determination of the quantum yields the ferrioxalate and KI/KIO$_3$ actinometers and a method for the calibration of radiometer detectors". Proc., 5th *Congress on Ultraviolet Technologies*, Amsterdam, the Netherlands.

Chu, L. and Anastasio, C. (2005) Formation of hydroxyl radical from the photolysis of

frozen hydrogen peroxide. *Journal of Physical Chemistry A. 109*, 6264-6271.

Feng, Y., Smith, D. W., and Bolton, J. R. (2007). Photolysis of aqueous free chlorine

species (NOCI and OCl⁻) with 254 nm ultraviolet light. *Journal of Environmental*

Engineering and Science, 6(3), 277-284.

Goldstein, S., Aschengrau, D., Diamant, Y., and Rabani, J. (2007). "Photolysis of

aqueous H_2O_2: Quantum yield and applications for polychromatic UV actinometry in

photoreactors." Environmental Science& Technology, 41, 7486-7490.

Nash, T. (1953). "The colorimetric estimation of formaldehyde by means of the Hantzsch

Reaction." J. Biochem., 55(3), 416-421.

CHAPTER 4 COMPARISON OF THE UV/CHLORINE AND THE UV/H$_2$O$_2$ PROCESSES FOR THE OXIDATION OF ORGANIC COMPOUNDS

4.1   Introduction

In Chapter 3, methanol was selected as the organic compound to investigate the UV/Chlorine and the UV/H$_2$O$_2$ processes. In order to investigate further the properties of the UV/Chlorine process and to compare to those of the UV/H$_2$O$_2$ process, further experiments were designed and carried out.

In this chapter, *para*-chlorobenzoic acid (*p*CBA) and cyclohexanoic acid (CHA) were selected as additional radical scavengers, and the first-order degradation rate constants and the photodegradation quantum yields of active chlorine were calculated and compared to those of the UV/H$_2$O$_2$ process.

To fulfill this purpose, the following experiments were designed and performed:

1. Examine the degradation of the probe compound (*para*-chlorobenzoic acid) using both the UV/Chlorine and the UV/H$_2$O$_2$ processes.

2. Calculate and compare the pseudo first-order reaction rate constants for *p*CBA degradation using both the UV/Chlorine and the UV/H$_2$O$_2$ processes.

3. Investigate the degradation of cyclohexanoic acid (CHA) using the UV/Chlorine process.

4. Determine the pseudo first-order reaction rate constant for the oxidation of CHA in the UV/Chlorine process and compare to that of the UV/H$_2$O$_2$ process.

4.2 Materials and Methods

4.2.1 Materials and equipment

The same equipment and materials were used for the experiments in this chapter as were introduced in Section 3.2.1.

For the photolysis of samples containing *para*-chlorobenzoic acid (*p*CBA), 99 % analytical reagent grade *p*CBA was obtained from Aldrich[®] (Canada). For the samples containing cyclohexanoic acid (CHA), 98% analytical reagent grade CHA was also obtained from Aldrich[®] (Canada).

The concentrations of *p*CBA solutions were measured by a high pressure liquid chromatography (HPLC) apparatus (Shimadzu, LC-10 AT VP) with a UV detector (Shimadzu, SPD-10 AVP). The concentrations of the CHA solutions were detected and measured by liquid chromatography-mass spectrometry (Varian 500 MS).

4.2.2 Preparation of samples

4.2.2.1 Preparation of samples containing para-chlorobenzoic acid (*p*CBA)

A bulk solution of *para*-chlorobenzoic acid solution was prepared and diluted for the chlorine or hydrogen peroxide samples containing *p*CBA.

To prepare the bulk solution, approximately 4.0 mg of *p*CBA was weighed on a microbalance and put into a 200 mL beaker containing approximately 200 mL MilliQ water. It was then put on a hot plate set to about 85 °C and stirred for approximately one hour (Zona *et al.,* 2010).

4.2.2.2 Preparation of samples containing cyclohexanoic acid (CHA)

The cyclohexanoic acid solutions were prepared by adding approximately 50 mg into 1 L volumetric flask filled with MilliQ water to yield a CHA concentration of 50 mg/L.

4.2.3 Sample measurements

4.2.3.1 Measurement of p-chlorobenzoic acid by reversed-phase HPLC

Reversed-phase high pressure liquid chromatography (HPLC) with a UV detector was used for the analysis of pCBA. Analysis was implemented using a 150 mm × 4.6 mm Gemini C18 (2) column with a 5 μm particle size (Phenomenex, Torrance, CA, USA). The mobile phase consisted of 45% 10 mM phosphoric acid and 55% methanol. The flow rate was set to 0.7 mL/min, and the sample injection volume was 100 μL (Vanderford *et al.*, 2007).

A standard curve for pCBA ranging from 1.3 to 10.2 μM was obtained and is shown in Figure 4.1.
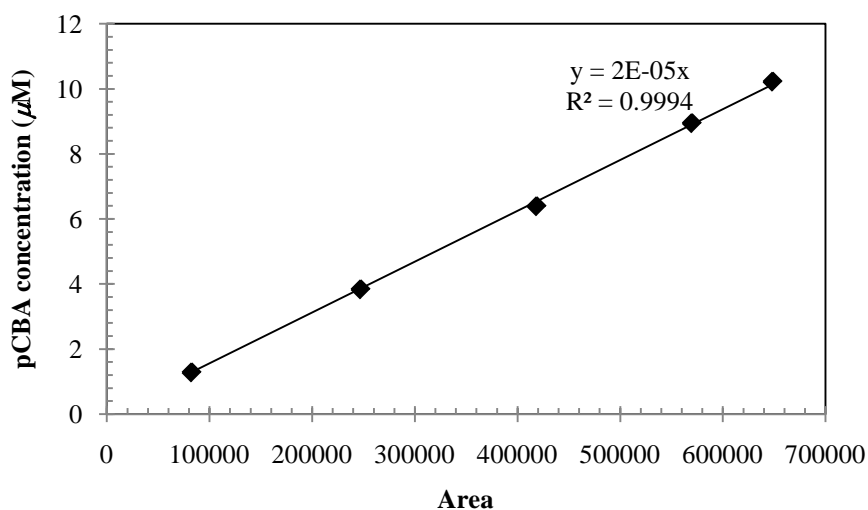
Figure 4.1 Standard curve for pCBA concentration measured by HPLC

4.2.3.2 Measurement of cyclohexanoic acid by liquid chromatography-mass spectrometry

An HPLC connected to an ion trap mass spectrometer (Varian 50-MS) equipped with an electrospray interface operating in negative ion mode, along with unit mass resolution, was used to detect and measure the CHA. An analytical Luna C8 (5 μm, 150 × 3 mm, and 250 × 3 mm) column was purchased from Phenomenex. The experimental temperature for the chromatography was about 40 °C. The mobile phase consisted of 100 % methanol containing 4 mM ammonium acetate and 0.1% acetic acid in aqueous solution. The concentration of methanol was ramped from 40 to 80% over 20 min. The mobile phase flow rate was 200 μL and the injection volume was 20 μL.

A standard curve for cyclohexanoic acid ranging from 0.04 − 0.4 mM was obtained and is shown in Figure 4.2.

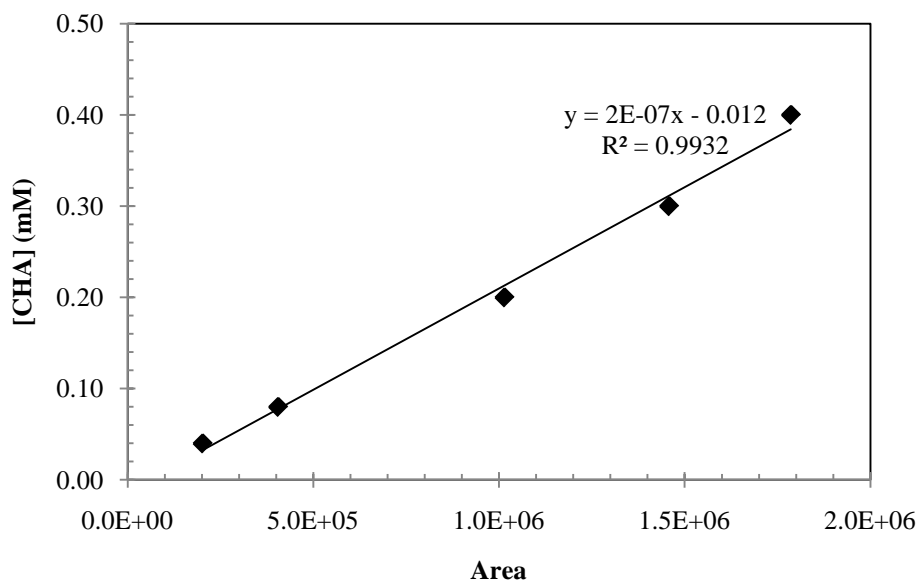Figure 4.2 Standard curve for cyclohexanoic acid concentration measured in LC MS

4.3   Results and Discussion

4.3.1   The oxidation of *para*-chlorobenzoic acid in the UV/Chlorine process

Samples were prepared with various *p*CBA concentrations to eliminate the possibility that the concentration of the organic compound might affect the reaction rate constant and the photodegradation quantum yields. Samples were prepared according to the methods given in Sections 3.2.2.1 and 4.2.2.1.

Two samples containing approximately 50 mg/L active chlorine and *p*CBA concentrations of 7.1 and 13.7 μM were prepared and exposed to UV for 600 – 3000 s, yielding UV doses of 228 – 1140 mJ/cm^2. The pH of the sample solutions was buffered to pH 5, since the photodegradation quantum yields and ·OH production rates are greater at pH 5 than at pH 10 for the UV/Chlorine process, as described in the latter part of Section 3.3.2. After each trial, the *p*CBA and active chlorine concentrations were determined by HPLC and the DPD method, respectively, as described in Sections 4.2.2.1 and 3.2.3.1.

Figure 4.3 shows plots of ln([*p*CBA]) versus the reaction time and the fit lines show the pseudo first-order reaction rate behaviour for *p*CBA reacting with ·OH radicals using the UV/Chlorine process. It can be observed from the figure that, although the initial concentrations of *p*CBA varied, the reaction rate constant remains about the same value, which indicates that the impact of the initial concentration of *p*CBA on the pseudo first-order reaction rate constant was minor.
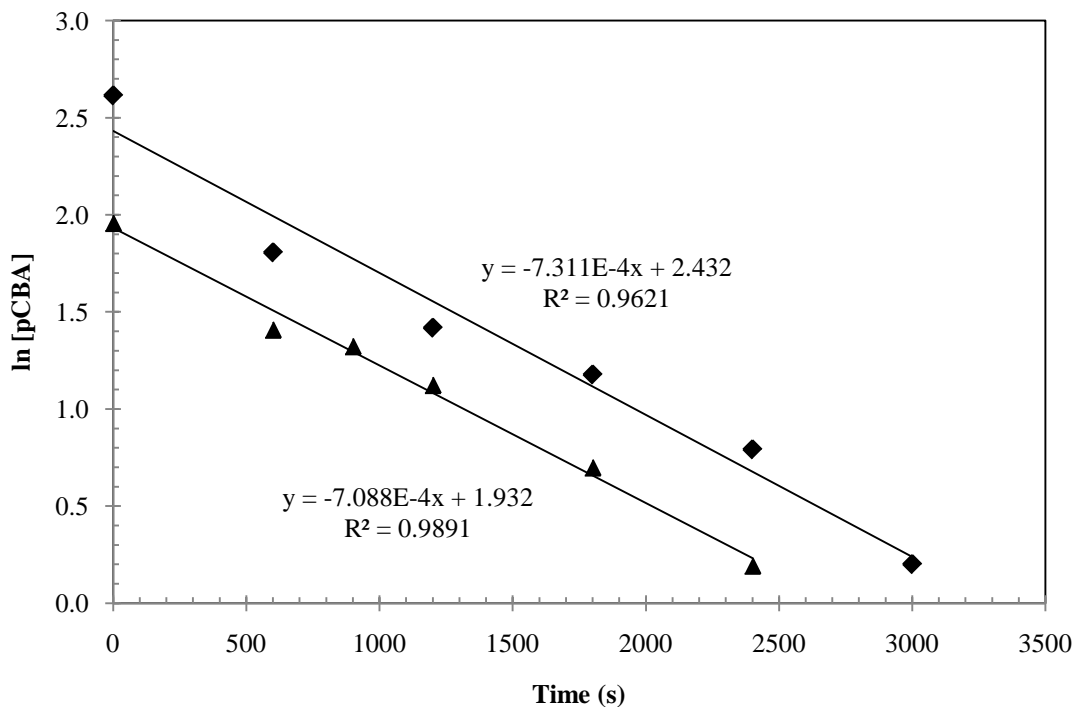
Figure 4.3 The pseudo first-order reaction rate constants for the *p*CBA being oxidized in the UV/Chlorine process.

Further investigation of *p*CBA oxidized by the UV/Chlorine process was carried out by adding methanol as an 'interfering' scavenger into chlorine solutions containing *p*CBA; hence, the impact of the methanol concentration on the reaction rate of *p*CBA with ·OH radicals was studied.

Three samples each containing approximately 50 mg/L active chlorine around pH 5 were prepared. Methanol was added to solutions to yield methanol concentrations of approximately 15, 40 and 99 mM, and the *p*CBA concentration for each sample was about 12.4, 10.0, and 14.3 μM, respectively. Since *p*CBA was dissolved into bulk solutions and then diluted for certain times to prepare the samples, it was hard to control the concentrations to be the same when preparing fresh bulk solutions each time before the trials. However, as discussed earlier in this section, the concentration of *p*CBA has

virtually no effect on the rate constants for pCBA reacting with ·OH radicals; hence, the various pCBA initial concentrations should not be of concern.

The samples so prepared were exposed under the LP UV lamp with an irradiance of 0.38 mW/cm^2 in a collimated beam apparatus for $240 - 1200$ s to yield UV doses of $91.2 - 456.0$ mJ/cm^2. After each trial, the active chlorine and pCBA concentrations were measured by the DPD method and by HPLC, respectively, as described in Sections 3.2.3.1 and 4.2.2.1.

The degradation rate constant of pCBA was lower in solutions with various methanol concentrations (mg/L), and the pseudo first-order reaction rate constants are shown in Figure 4.4. It could be observed that the rate constants decreased from 6.18×10^{-4} to 4.90×10^{-4} to 2.20×10^{-4} s^{-1} as the methanol concentrations increased from 15 to 40 to 99 mM, respectively. Also the rate constants were all lower than the 7.31×10^{-4} and 7.09×10^{-4} s^{-1}, values obtained when there was no methanol present, as illustrated in the earlier part of this section.
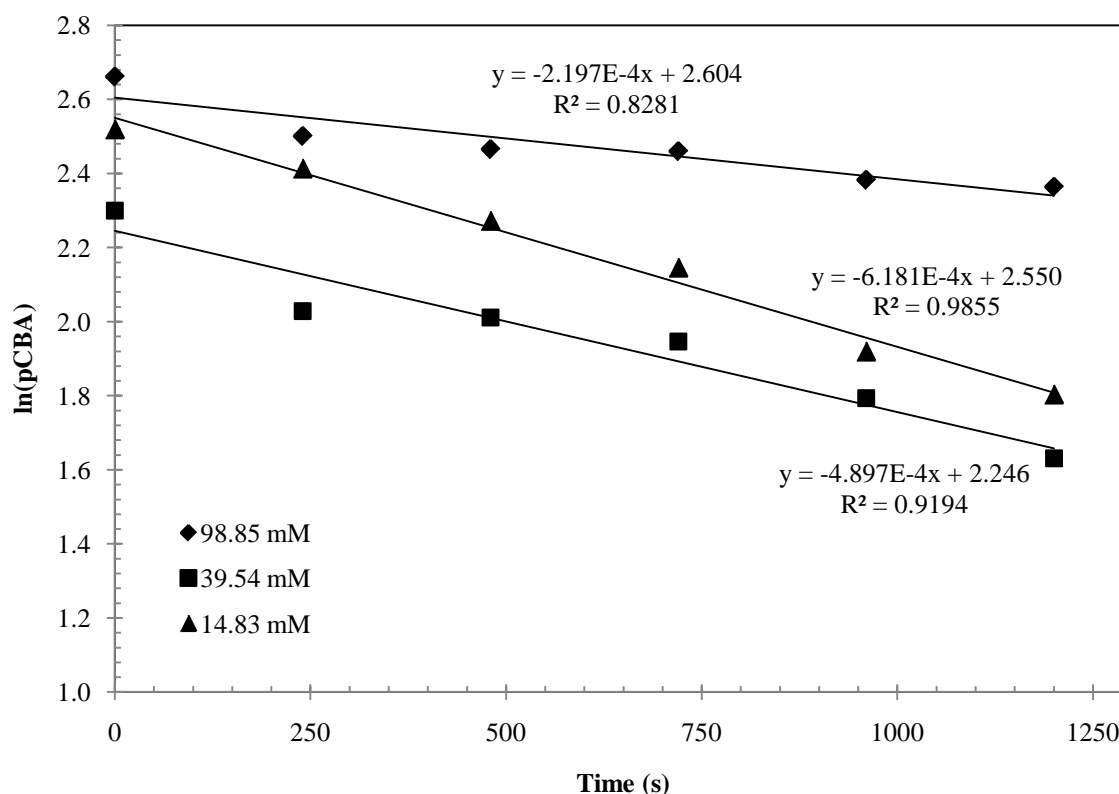
Figure 4.4 The pseudo first-order reaction degradation rate constants of *p*CBA in the presence of various methanol concentrations (mM) using the UV/Chlorine process.

Figure 4.5 shows a better demonstration of the decrease of the pseudo first-order reaction rate constants (s^{-1}) of *p*CBA in the presence of methanol in the UV/Chlorine process.

It can be inferred from Figure 4.5 that the pseudo first-order reaction rate constants (s^{-1}) decrease linearly with the slope of 4.96×10^{-6} with increasing methanol concentrations (mg/L).
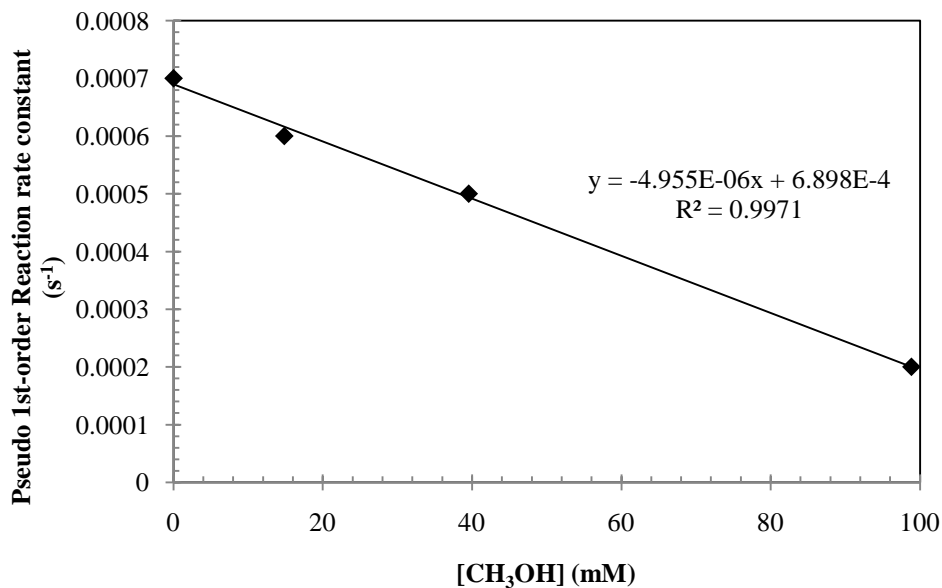
Figure 4.5 The relation between the pseudo first-order reaction rate constants (s^{-1}) for pCBA degradation and the methanol concentration (mM).

4.3.2   The oxidation of *para*-chlorobenzoic acid in the UV/H$_2$O$_2$ process

The UV/H$_2$O$_2$ trials were designed in parallel to those of the UV/Chlorine trials.

Cyclohaxanoic acid (CHA) and p-chlorobenzoic acid (pCBA) were also used as radical

scavengers for the investigation of the UV/H$_2$O$_2$ process.

Three samples were prepared containing approximately 200 mg/L H$_2$O$_2$ and 5.3, 9.4 and

14.6 μM pCBA, and were labeled as Sample 1, Sample 2, and Sample 3, respectively.

For Sample 3, methanol was added to yield a concentration of approximately 40 mM, to

investigate whether methanol will interfere with the oxidation of pCBA in the UV/H$_2$O$_2$

process similar to that of the UV/Chlorine process.

The samples were then exposed to the LP UV lamp in the collimated beam apparatus for

180 – 900 s receiving UV doses varying from 114 to 570 mJ/cm^2. After each trial, the

pCBA and H$_2$O$_2$ concentrations were determined according to Sections 3.2.3.1 and

3.2.3.4. The photodegradation quantum yields of H$_2$O$_2$ and the pseudo first-order reaction

74

rate constants for the degradation of pCBA by ·OH radicals were then calculated; the decay curves and rate constants are shown in Figure 4.6.

It can be easily concluded from Figure 4.6 that the initial concentration of pCBA has no impact on the reaction rate constants. Furthermore, the addition of methanol greatly reduced the oxidation rate of pCBA using the UV/H$_2$O$_2$ process by reducing the pseudo first-order rate constant of pCBA from 1.9×10^{-3} to 3.9×10^{-4} s^{-1}, similar to that for the UV/Chlorine process.
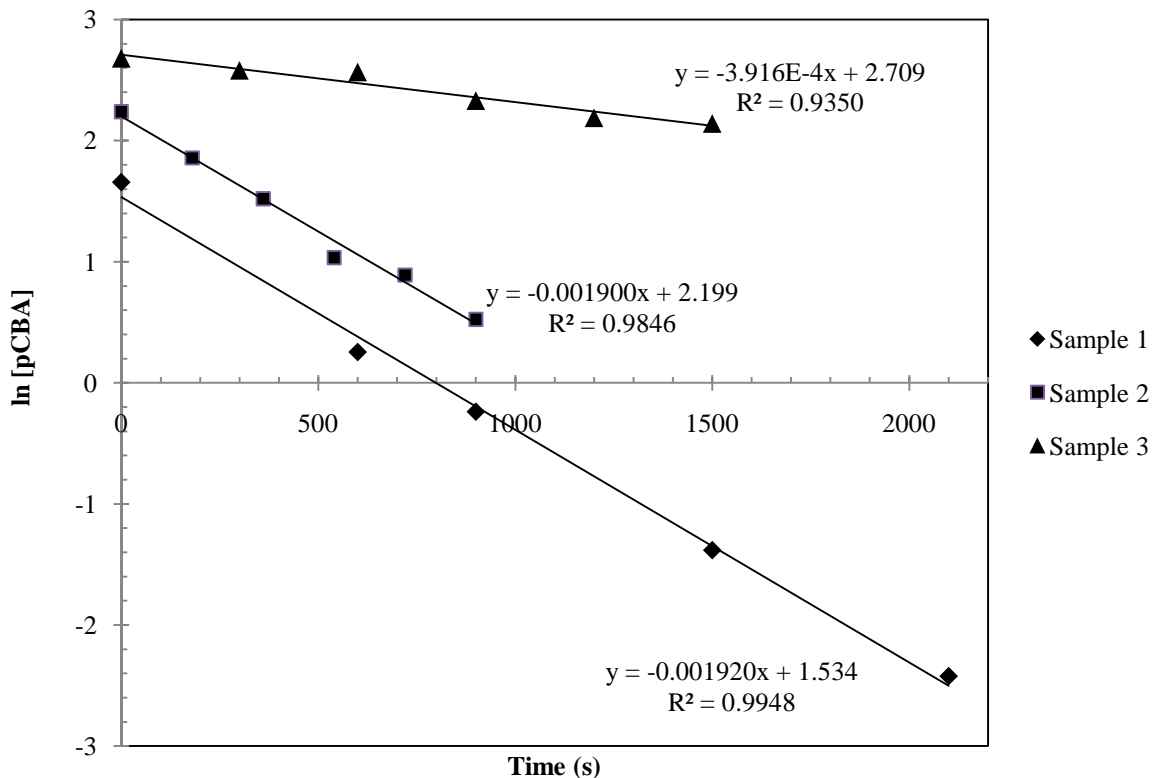

Figure 4.6 Pseudo first-order reaction rate constants of pCBA for various methanol concentrations (mM) during the UV/H$_2$O$_2$ process.

4.3.3   Specific rate constants for the degradation of pCBA

Since the aqueous chlorine and hydrogen peroxide components have different absorbances at 254 nm when samples are exposed to LP UV, the fraction of UV absorbed

by the samples is different in each case. Thus, when comparing the pseudo first-order

reaction rate constants of pCBA in the UV/Chlorine and the UV/H$_2$O$_2$ processes, the rate

constants should be converted to 'specific rate constants', since the chlorine and

hydrogen peroxide solutions have different absorbances at 254 nm.

The pseudo first-order reaction rate constant obtained was converted to a 'specific rate

constant' by dividing by the fraction of UV absorbed. The conversion process was as

follows:

Eq. (4.1) $$k(\text{specific}) = k/[1 - 10^{(-A_{254})}]$$

where:

    k(specific) = the 'specific' pseudo first-order reaction rate constant (s^{-1}) at 254 nm

    k = the experimental reaction rate constant (s^{-1}) calculated directly from a plot of

    ln([pCBA]) versus time (s)

    A_{254} = the absorbance of the chlorine sample containing pCBA

In effect, the specific rate constant is the rate constant that would be obtained if all of the

UV would be absorbed.

Since the average k (s^{-1}) for the active chlorine samples containing pCBA without

methanol at pH 5 was $(7.20 \pm 0.11) \times 10^{-4}$ s^{-1} (from Figure 4.3), the k(specific) for pCBA

degradation in the UV/Chlorine process was calculated to be $(5.67 \pm 0.09) \times 10^{-3}$ s^{-1}.

Also the specific pseudo first-order reaction rate for the H$_2$O$_2$ samples containing pCBA

without methanol was calculated according to Eq. (4.1). The k(specific) was for pCBA

76

degradation in the UV/H$_2$O$_2$ process was $(9.91 \pm 0.05) \times 10^{-3}$ s^{-1}. This specific rate

constant for the degradation of pCBA in the UV/H$_2$O$_2$ process is higher than that of the

UV/Chlorine process [k(specific) = $(5.67 \pm 0.09) \times 10^{-3}$ s^{-1}].

4.3.4   Oxidation of cyclohexanoic acid using the UV/Chlorine photolysis

Following the examination of the oxidation of pCBA, cyclohexanoic acid (CHA) was

added into chlorine solutions in order to further investigate the UV/Chlorine process.

Samples were prepared containing approximately 50 mg/L chlorine at pH 5 and 0.540

mM CHA and were exposed under the LP UV lamp at an irradiance of 0.38 mW/cm^2 in a

collimated beam apparatus for 1200, 1800, 2400, 3000 and 3600 s. After each trial, the

CHA and active chlorine concentrations were measured according to the methods in

Sections 4.2.3.2 and 3.2.3.1.

Figure 4.7 shows the degradation and the pseudo first-order reaction rate constants for the

oxidation of CHA using the UV/Chlorine process.
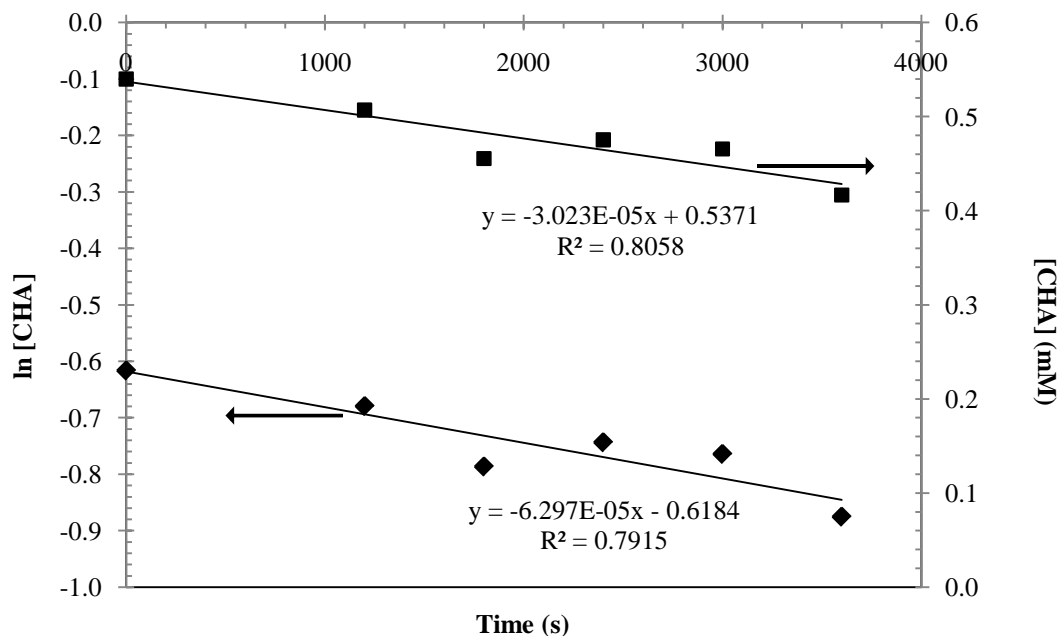
Figure 4.7 Degradation of cyclohexanoic acid in the UV/Chlorine process

As shown in Figure 4.7, it can be easily seen that the CHA did not degrade very rapidly

during the process. The pseudo first-order reaction rate constant for CHA was only (6.30

$\pm 0.3) \times 10^{-5}$ s^{-1}. The 'specific' pseudo first-order reaction rate constant at 254 nm was

also calculated for the degradation of CHA in the UV/Chlorine process, and the value

was $(1.39 \pm 0.06) \times 10^{-3}$ s^{-1}, which is relatively small compared to that of pCBA

degradation in the UV/Chlorine process.

4.4   Conclusions

In this chapter, the experiments began by adding various concentrations of p-

chlorobenzoic acid (pCBA) into chlorine samples and observing the degradation of the

compound.

Active chlorine samples (at pH 5) containing 7.1 mM and 13.7 μM pCBA were exposed

to LP UV for 600 $-$ 3000 s, and the pCBA and chlorine concentrations in the samples

were measured to calculate the degradation of pCBA. It can be concluded from the results that, in spite of various initial pCBA concentrations, the pseudo first-order reaction rate constant for pCBA using the UV/Chlorine process stayed constant at $(7.20 \pm 0.11) \times 10^{-4}$ s^{-1}, indicating that the pCBA initial concentration has no effect on the reaction rate constant.

The results from Chapter 3 showed that methanol greatly increased the production of $\cdot$OH radicals in the UV/Chlorine process. Thus, to investigate whether methanol could stimulate better degradation of pCBA in the UV/Chlorine process, methanol along with pCBA was added to chlorine samples.

Samples containing 14.3 mM pCBA and various methanol concentrations were prepared and exposed to UV in the UV collimated beam apparatus for $240 - 1200$ s. The results showed that, rather than accelerating the degradation of pCBA, methanol become the principal competitor for $\cdot$OH radicals, and the pseudo first-order reactions rate constant for the degradation of pCBA was decreased by the addition of methanol. The rate constant decreased from 7.20×10^{-4} s^{-1} (with no addition of methanol) to 6.18×10^{-4} 4.90×10^{-4} to 2.20×10^{-4} s^{-1} when the methanol concentration increased from 15 to 40 to 99 mM, respectively. Further calculation indicated that the rate constants for the degradation of pCBA decreased linearly as the methanol dose increased.

Parallel experiments were conducted in the UV/H_2O_2 process as well. Results showed that the pseudo first-order rate constant for the degradation of pCBA stayed the same being 1.91×10^{-3} s^{-1}, regardless of the various initial concentrations of pCBA. Furthermore, the addition of approximately 40 mM methanol into the sample solutions

also showed an inhibiting effect on the degradation of pCBA by lowering the reaction rate constant to 3.92×10^{-4} s^{-1} when approximately 40 mM methanol was added.

The experiments on the oxidation pCBA showed that methanol, rather than being an accelerator during the UV/Chlorine and the UV/H$_2$O$_2$ processes, became the dominant radical scavenger. And more importantly, the UV/H$_2$O$_2$ process showed a higher efficiency in oxidizing pCBA. Chain reactions were not triggered by pCBA during the UV/Chlorine process, as compared to when methanol was introduced into the UV/Chlorine process and achieved better performance in oxidizing methanol.

Besides pCBA, cyclohexanoic acid (CHA) was also added to chlorine solutions to further investigate the UV/Chlorine process. Samples containing 50 mg/L chlorine and 0.534 mM CHA were exposed to LP UV lamp for 1200, 1800, 2400, 3000, 3600 s. The CHA and chlorine concentrations were monitored for further calculation of the results. The CHA only degraded slowly during the UV/Chlorine process, indicating that the process might not suitable for the degradation of CHA.

4.5   References

Vanderford, B. J., Rosario-Ortiz, F. L., and Snyder, S. A. (2007). "Analysis of p-chlorobenzoic acid in water by liquid chromatography-tandem mass spectrometry." *J. Chromatography Analysis,* 1164(1-2), 219-223.

Zona, R., Solar, S., Getoff, N., Sehested, K., and Holcman, J. (2010). "Reactivity of OH radicals with chlorobenzoic acids-A pulse radiolysis and steady-state radiolysis study." *Radiat. Phys. Chem.,* 79(5), 626-636.

CHAPTER 5 GENERAL CONCLUSIONS

5.1   General overview

As discussed in Chapter 1, the application of UV technologies in water and wastewater treatment has become more and more popular. The UV/Chlorine process, which can generate the strong oxidizing substance (·OH radicals), has been studied in recent years as one of the Advanced Oxidation Processes (AOPs).

This research began by a thorough study of the theory of UV/Chlorine photolysis. The equations to calculate the quantum yield of active chlorine and the yield factor were discussed. Factors, such as pH, concentration of active chlorine, temperature, the presence of organic matter and wavelength, which influence the quantum yields were also discussed. The theory of the UV/Chlorine process was introduced to better understand the process and was applied in further calculations of the data obtained. The factors influencing the quantum yields were important in the design of the experiments and in quality control and assurance.

Meanwhile, the research also discussed the possible applications of the UV/Chlorine process as studied by several scholars. Feng *et al.,* (2010) studied the fluence (UV dose) delivered by a UV reactor by the Photolysis of Active Chlorine (PAC) method, and compared the results to those of a biodosimetry test for the validation of UV reactors. As a result, the fluence delivered in the reactor measured by PAC method was similar to that of biodosimetry method. The PAC method, as one of the applications of the UV/Chlorine process, was proved in this study to be very efficient and reliable.

Watts *et al.,* (2007) studied the degradation of *para*-chlorobenzoic acid (*p*CBA) and nitrobenzene (NB) in the UV/Chlorine process and calculated the rate constants for the *p*CBA and NB probes reacting with ·OH radicals. They reported that the ·OH radical scavenging rate was $8.46 \times 10^4 \, M^{-1} \, s^{-1}$, which is smaller than the rate in the UV/H_2O_2 process, being $2.7 \times 10^7 \, M^{-1} \, s^{-1}$ (Buxton *et al.,* 1988). This fact indicates that the UV/Chlorine process might be a more efficient AOP than the UV/H_2O_2 process in the oxidation of organic compounds. Thus, this research mainly aimed to study the efficiency of the UV/Chlorine process in oxidizing several organic compounds and compared the results to those of the UV/H_2O_2 process to evaluate the potential of the UV/Chlorine process being utilized in the water and wastewater treatment industry.

5.2   Conclusions

Results were obtained based on the experiments carried out in previous chapters. A general summary of the whole research is as follows.

5.2.1   Photodegradation quantum yield of active chlorine at pH 5

Experiments carried out by Feng *et al.,* (2007) were repeated at the beginning of the research to assure that the experimental designs and techniques were proper. Photodegradation quantum yields of up to 90 mg/L active chlorine at pH 5 were obtained. The values were 1.03 ± 0.11 and were similar to the results by Feng *et al.,* (2007).

5.2.2   Photodegradation quantum yield of active chlorine at pH 5 and 10

Methanol was added to active chlorine solutions at pH 5 and 10 and the photodegradation quantum yields were calculated. Apparently chain reactions occurred at pH 5 in the presence of methanol, since the quantum yield increased from 3.6 up to 16.6 mol einstein⁻

[1] when methanol dose changed from 9.9 to 86.5 mM. However, the photodegradation quantum yields of active chlorine at pH 10 showed no change and stayed at 1.15 ± 0.08. The results indicate when OCl^- dominates in the solution, there was no occurrence of chain reactions.

5.2.3 Quantum yield of the production of ·OH radicals in the UV/H₂O₂ process

The quantum yield of production of ·OH radicals was calculated in the UV/H_2O_2 process. In spite of an increasing methanol dose, the quantum yield stayed at about 1.13 ± 0.12 mol einstein^{-1}. The results proved that the addition of methanol cannot trigger chain reactions unlike active chlorine solutions at pH 5.

5.2.4 Generation of ·OH radicals in the UV/Chlorine process

The production of ·OH radicals can be quantified by measuring the concentration of formaldehyde that was produced as methanol was oxidized. The formaldehyde production increased as the methanol dose increased, and became stabilized when the methanol dose reached about 25 mM. The yield factor of active chlorinate at pH 5 for generating ·OH radicals was 0.46± 0.09.

5.2.5 Generation of ·OH radicals in the UV/H₂O₂ process

Similar to the results obtained in the UV/Chlorine process, the formaldehyde production increased as the methanol dose increased and became stable when the methanol concentration reached about 10 mM. However, the yield factor increased and reached about 1.0 unlike the case of the UV/Chlorine process, where the yield factor stayed constant at 0.46± 0.09.

5.2.6 Degradation rate constants of *p*CBA being oxidized in the UV/Chlorine process

Pseudo first-order degradation rate constants of *p*CBA being oxidized in the UV/Chlorine process were not affected by the initial concentration of *p*CBA and stayed constant at 7.20×10^{-4} s^{-1}. However, when methanol was added into the *p*CBA samples, the rate constants decreased with a slope of 4.96×10^{-6}. It can be concluded that methanol acted as a competing species against *p*CBA for ·OH radicals.

5.2.7 Degradation rate constants of *p*CBA being oxidized in the UV/H$_2$O$_2$ process

Similar experiments were carried out in the UV/H$_2$O$_2$ process. Again, the initial *p*CBA concentration had no effect on the pseudo first-order degradation rate constant. The addition of methanol decreased the rate constant similar to the results obtained in the UV/Chlorine process. A specific rate constant for the degradation of *p*CBA was calculated and compared the corresponding specific rate constant in the UV/H$_2$O$_2$ process, where specific rate constant was $(9.91 \pm 0.05) \times 10^{-3}$ s^{-1}, significantly larger than that for the UV/Chlorine process, which was $(5.67 \pm 0.09) \times 10^{-3}$ s^{-1}.

5.2.8 Degradation rate constants of CHA being oxidized in the UV/Chlorine process

The results showed that CHA can be oxidized only slowly by the UV/Chlorine process, where the 'specific' pseudo first-order reaction rate constant for CHA was only $(1.39 \pm 0.06) \times 10^{-3}$ s^{-1} and was considerably smaller than that of the UV/H$_2$O$_2$ process according to the results obtained by Afzal *et al.,* (2010) which was 0.014 s^{-1}.

The results in this research indicated that although chain reactions occur in active chlorine solutions at pH 5, and the photodegradation quantum yields are larger in the UV/Chlorine process at pH 5 in the presence of methanol, the yield of factor for the generation of ·OH radicals was smaller in the UV/Chlorine process as compared to the UV/H_2O_2 process. Meanwhile, the specific degradation reaction rate constants of pCBA and CHA being oxidized in the UV/Chlorine process were not as high as those of the UV/H_2O_2 process, indicating that the UV/Chlorine process is not as efficient as the UV/H_2O_2 process in oxidizing these organic substances. However, more investigation should be carried out to further evaluate the potential of the UV/Chlorine process.

5.3   References

Buxton, G. V., Greenstock, C. L., Helman, W. P., and Ross, A. B. (1988). "Critical-Review of Rate Constants for Reactions of Hydrated Electrons, Hydrogen-Atoms and Hydroxyl Radicals (·OH/·O$^-$) in Aqueous-Solution." Journal of Physical and Chemical Reference Data, 17(2), 513-886.

Feng, Y., Smith, D. W., and Bolton, J. R. (2010). "A Potential New Method for Determination of the Fluence (UV Dose) Delivered in UV Reactors Involving the Photodegradation of Free Chlorine." Water Environ. Res., 82(4), 328-334.

Feng, Y., Smith, D. W., and Bolton, J. R. (2007). "Photolysis of aqueous free chlorine species (NOCI and OCI-) with 254 nm ultraviolet light." Journal of Environmental Engineering and Science, 6(3), 277-284.

Watts, M. J., and Linden, K. G. (2007). "Chlorine photolysis and subsequent OH radical production during UV treatment of chlorinated water." Water Res., 41(13), 2871-2878.